AD-A057 304 KENTUCKY UNIV LEXINGTON DEPT OF ENGINEERING MECHANICS F/G 12/1
THE BOUNDARY INTEGRAL EQUATION METHOD FOR THE NUMERICAL SOLUTIO--ETC(U)
APR 78 M L SCHULOCK AFOSR-75-2824
UNCLASSIFIED UKY-TR107-78-EM16 AFOSR-TR-78-1184 NL

1 OF 2
ADA
057304

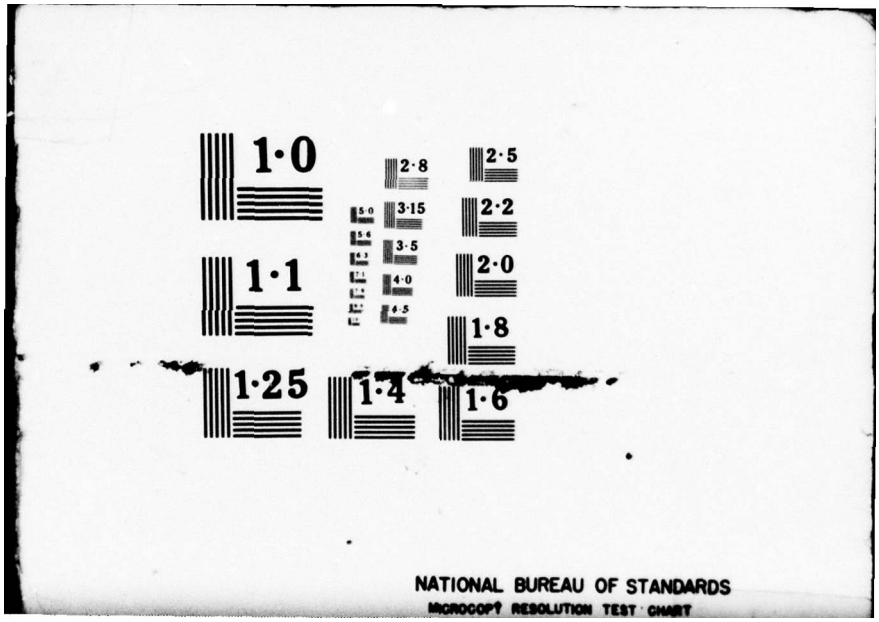
1·0
1·1
1·25
2·8
3·15
3·5
4·0
4·5
5·0
2·5
2·2
2·0
1·8
1·4
1·6
NATIONAL BUREAU OF STANDARDS
MICROCOPY RESOLUTION TEST CHART

REPORT DOCUMENTATION PAGE

READ INSTRUCTIONS BEFORE COMPLETING FORM

1. REPORT NUMBER: AFOSR-TR-78-1184
2. GOVT ACCESSION NO.
3. RECIPIENT'S CATALOG NUMBER

4. TITLE (and Subtitle)
THE BOUNDARY INTEGRAL EQUATION METHOD FOR THE NUMERICAL SOLUTION OF BOUNDARY VALUE PROBLEMS GOVERNED BY SECOND ORDER ELLIPTIC EQUATIONS

5. TYPE OF REPORT & PERIOD COVERED
INTERIM

6. PERFORMING ORG. REPORT NUMBER
UKY TR107-78-EM16

7. AUTHOR(s)
MICHAEL L SCHULOCK

8. CONTRACT OR GRANT NUMBER(s)
AFOSR 75-2824

9. PERFORMING ORGANIZATION NAME AND ADDRESS
UNIVERSITY OF KENTUCKY
DEPARTMENT OF ENGINEERING MECHANICS
LEXINGTON, KENTUCKY 40506

10. PROGRAM ELEMENT, PROJECT, TASK AREA & WORK UNIT NUMBERS
2307B1
61192F

11. CONTROLLING OFFICE NAME AND ADDRESS
AIR FORCE OFFICE OF SCIENTIFIC RESEARCH/NA
BLDG 410
BOLLING AIR FORCE BASE, D C 20332

12. REPORT DATE
April 1978

13. NUMBER OF PAGES
107

14. MONITORING AGENCY NAME & ADDRESS (if different from Controlling Office)

15. SECURITY CLASS. (of this report)
UNCLASSIFIED

15a. DECLASSIFICATION/DOWNGRADING SCHEDULE

16. DISTRIBUTION STATEMENT (of this Report)
Approved for public release; distribution unlimited.

17. DISTRIBUTION STATEMENT (of the abstract entered in Block 20, if different from Report)

18. SUPPLEMENTARY NOTES

19. KEY WORDS (Continue on reverse side if necessary and identify by block number)
BOUNDARY VALUE PROBLEMS
BOUNDARY INTEGRAL EQUATION METHOD
ANISOTROPIC HEAT CONDUCTION
ANISOTROPIC ELASTICITY

20. ABSTRACT (Continue on reverse side if necessary and identify by block number)
A new, general, boundary-integral-equation procedure for the numerical solution of boundary value problems governed by second order elliptic equations is implemented. Boundary geometry and dependent variables are approximated by means of quadratic shape functions. The procedure is applied to plane problems of anisotropic heat conduction and anisotropic elasticity. Comparisons between exact and numerical solutions are given.

DD FORM 1 JAN 73 1473

(18) AFOSR

AFOSR- (19) AFOSR-TR- 78-1184

(14) UKY-TR107-78-EM16

(6) THE BOUNDARY INTEGRAL EQUATION METHOD FOR THE NUMERICAL SOLUTION OF BOUNDARY VALUE PROBLEMS GOVERNED BY SECOND ORDER ELLIPTIC EQUATIONS .

(9) Special Scientific Report,

(16) 2307

(17) B1

(10) Michael L. Schulock
Department of Engineering Mechanics
University of Kentucky
Lexington, Kentucky 40506

(11) April 1978

(12) 108p.

Approved for Public Release
Distribution Unlimited

Prepared For
Air Force Office of Scientific Research
Bolling Air Force Base
Washington, D.C. 20332

(15) AFOSR-75-2824

AIR FORCE OFFICE OF SCIENTIFIC RESEARCH (AFSC)
NOTICE OF TRANSMITTAL TO DDC
This technical report has been reviewed and is
approved for public release IAW AFR 190-12 (7b).
Distribution is unlimited.
A. D. BLOSE
Technical Information Officer

TABLE OF CONTENTS

TABLE OF CONTENTS (CONTINUED)

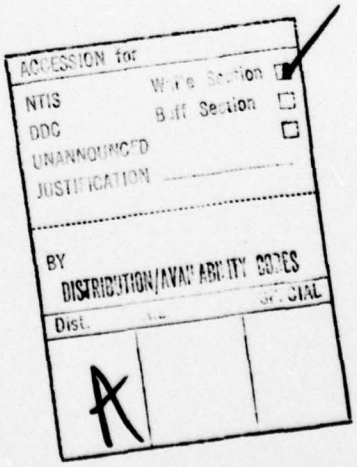

LIST OF FIGURES

LIST OF TABLES

CHAPTER ONE

INTRODUCTION

The need to solve boundary value problems of mathematical physics has always been appreciated. From the outset, enough assumptions were made to arrive at a solution which approximated the physical behavior of the problem in question. As the geometry of the problem became complex, approximations in the solution procedure were accepted to arrive at a final result, leading to graphical and numerical solution techniques. Irreconcilably, only certain classes of problems were admitted within these techniques, which were basically determined by the assumptions alluded to at the outset. The goal of approximating physical behavior of this class of problems more closely or of any problem not within the class can only be realized by a reexamination of the underlying assumptions, leading to more complex governing differential equations. It follows that the solution of these governing equations when considered over any geometry other than the most rudimentary becomes cumbersome and even unobtainable analytically, while the graphical approach becomes eliminated altogether, leaving the numerical technique as the apparent means of solution.

The numerical technique is flexible since it is applicable to systems of varying properties and nonuniform boundary conditions besides being adaptable to complex

geometry. While the numerical technique involves complicated and tedious manipulations, high-speed, large-capacity digital computers have been developed to accomodate them. Although numerical methods do not provide general solutions, this could be of little consequence, because it may be the particular solution which is of practical interest. In fact, when the general solution is available, it might prove to be difficult and tedious to translate it to a particular solution.

Numerical techniques have a rich history and have been extensively and successfully applied to the title boundary value problems in the form of finite difference methods (FDM) and finite element methods (FEM). There are also practical difficulties associated with these methods which are also well known [1]. The fact that we are dealing with elliptic partial differential equations deserves special consideration. It is this fact in combination with natural constraints on physical constants that allows us to relate interior variables to boundary variables, which is the essence of the BIE method. This means that only the boundary of the problem need be dealt with -- a reduction of the dimensions of the problem by one. Furthermore, only interior variables of interest need be evaluated if desired. In order to effect the BIE method, a fundamental singular solution of the governing differential equations must be found, which when combined with

the desired solution through a reciprocal relation that will be derived leads to integral equations defined on the boundary of the problem domain. While this represents an exact means of solving the system, it is adapted to an approximate numerical procedure by a sufficient number of approximations within the integral equations to convert them to ordinary equations in unknown boundary data. These equations contain integrals of relevant variables in which the integrals are generally attacked numerically.

This thesis will deal with the application of the BIE method to systems of second order elliptic linear partial differential equations.

In Chapter Two, we formulate the BIE for the title problems and indicate both the general numerical procedure and specifically a polynomial shape function (PSFBIE) numerical procedure. The details of relevant limit processes needed for the establishment of the BIE are given in Appendix I. The details of the calculation of the matrix of coefficients used in the solution for unknown boundary data for a polynomial shape function BIE (PSFBIE) with Legendre Gauss quadrature of relevant integrals is given in Appendix II. Whereas these items are appendicized to allow formulative ideas to flow, they constitute the basis for actual numerical solutions.

In Chapter Three, the method is applied to two specific second order linear elliptic systems - anisotropic heat conduction and elasticity. Problems of physical

significance in two-dimensions are solved via the BIE method and are compared with analytical solutions, when available, to illustrate the features and reliability of the method.

In Chapter Four, we offer some discussion and conclusions regarding the method in general and some of the approximations made to convert the BIE to a numerical procedure.

CHAPTER TWO

BOUNDARY INTEGRAL EQUATION FOR BOUNDARY VALUE PROBLEMS GOVERNED BY SECOND ORDER ELLIPTIC SYSTEMS

2.1 ELLIPTIC PARTIAL DIFFERENTIAL EQUATIONS

2.1.1 Boundary Value Problems

The theoretical development of the method has been given in general form by Clements and Rizzo [2]. The first three sections of this chapter are essentially a reproduction of material presented in their paper.

Consider the problem of determining a system of functions $\phi_k(x_j)$, (k=1,2,...N, j=1,2) throughout a two-dimensional region R where ϕ_k satisfies

$$a_{ijk\ell} \frac{\partial^2 \phi_k}{\partial x_j \partial x_\ell} = 0 \qquad \begin{matrix} i,\ k = 1,\ 2,\ldots N \\ j,\ \ell = 1,\ 2 \end{matrix}$$

$$x_j \in R \tag{2.1}$$

and R is a simply or multiply connected domain with boundary C. (The summation convention is implied on all lower case Latin indices.)

We impose further that the $a_{ijk\ell}$ in (2.1) are real constants satisfying the symmetry condition

$$a_{ijk\ell} = a_{k\ell ij} \tag{2.2}$$

The ellipticity requirement can be expressed by

$$a_{ijk\ell} \frac{\partial \phi_i}{\partial x_j} \frac{\partial \phi_k}{\partial x_\ell} > 0 \qquad (2.3)$$

for arbitrary non-zero $\partial \phi_i / \partial x_j$, $\partial \phi_k / \partial x_\ell$.

We wish to find a solution to (2.1) which is valid in the two dimensional region R with boundary C. The problem is posed with the dependent variables ϕ_k or P_i specified on C, where

$$P_i = a_{ijk\ell} \frac{\partial \phi_k}{\partial x_\ell} n_j \qquad (2.4)$$

in which n_j is the unit outward normal to C. In other words the boundary conditions can be either of the form (Dirichlet type)

$$\phi_k(x_j) = f_k(x_j) \qquad (x_j) \in C$$

or of the form (Neuman type)

$$P_i(x_j) = g_i(x_j) \qquad (x_j) \in C$$

or of the form (Mixed problem)

$$\phi_k(x_j) = f_k(x_j) \qquad (x_j) \in C_1$$

$$P_i(x_j) = g_i(x_j) \qquad (x_j) \in C_2$$

where $C = C_1 \cup C_2$. The functions $f_k(x_j)$ and $g_i(x_j)$ are prescribed on the boundary C, and in accordance with a well posed boundary value problem, $f_k(x_j)$ and $g_i(x_j)$ are not simultaneously prescribed over the same part of the boundary.

If the problem is of the second type, ($P_i(x_j)$ specified on C), we require

$$\int_C P_i dS = 0 \tag{2.5}$$

which represents a steady-state restriction in the scalar case of N=1 and static equilibrium for N>1.

2.1.2 Solution In Terms of Analytic Functions

An analytic solution, by its nature, allows us to take derivatives of the fundamental variable ϕ_k to determine P_i via the constitutive relation (2.3) - making the boundary integral equation formulation more concise. Accordingly, we may take the form of the solution of (2.1) as

$$\phi_k = A_k f(z) \tag{2.6}$$

in which $f(z)$, $z \equiv x_1 + px_2$, is an analytic function of the variable z to be determined while A_k and p are constants. Substitution of (2.6) into (2.1) yields the homogenous algebraic system of N equations

$$(a_{i1k1} + a_{i1k2}p + a_{i2k1} + a_{i2k2}p^2)A_k = 0 \qquad (2.7)$$

which presents a characteristic value problem if the solution is to be non-trivial. Accordingly, this requires that

$$\left| a_{i1k1} + a_{i1k2}p + a_{i2k1}p + a_{i2k2}p^2 \right| = 0 \qquad (2.8)$$

The determinant in (2.8) gives rise to a polynomial of degree of 2N in p, which has N roots, which will be required to be distinct. These N roots are necessarily complex, in order that they satisfy the ellipticity condition (2.3). Eshelby et al [3] prove that the ellipticity condition is violated for a real root for the case of N=3. Furthermore, because the $a_{ijk\ell}$ are real it follows that the roots will occur in complex conjugate pairs.

Denoting those roots with positive imaginary parts by p_α, $\alpha = 1,2,\ldots N$, and their conjugates by $\bar{p}_\alpha$, the corresponding A will be identified as $A_{k\alpha}$ and $\bar{A}_{k\alpha}$, respectively. The real solution of (2.1) can then be written as

$$\phi_k = \sum_{\alpha=1}^{N} A_{k\alpha} f_\alpha(z_\alpha) + \sum_{\alpha=1}^{N} \bar{A}_{k\alpha} \bar{f}_\alpha(\bar{z}_\alpha) \qquad (2.9)$$

where $z_\alpha \equiv x_1 + p_\alpha x_2$.

2.1.3 A Reciprocal Relation Between Boundary and Interior Values

The reciprocal relation which we develop here results from an application of Green's Theorem to the governing differential equation (2.1) which we will later use in conjunction with a fundamental singular solution ϕ_k to develop an interior identity. The application of Green's Theorem is accomplished by letting ϕ_k be a solution of

$$a_{ijk\ell} \frac{\partial^2 \phi_k}{\partial x \, \partial x_\ell} = h_i(x_1, x_2) \qquad (2.10)$$

with corresponding P_k as defined by (2.4). Also let ϕ_k' be a solution to a similar system with h_i replaced by h_i'. By the definition of P_k and the divergence theorem, we may write

$$\int_C P_i \phi_i' ds \equiv \int_C a_{ijk\ell} \frac{\partial \phi_k}{\partial x_\ell} n_j \phi_i' ds$$

$$= \int_R a_{ijk\ell} \frac{\partial}{\partial x_j} \left(\frac{\partial \phi_k}{\partial x_\ell} \phi_i' \right) dR \qquad (2.11)$$

Using (2.10), this becomes

$$\int_C P_i \phi_i' dS = \int_R a_{ijk\ell} \frac{\partial \phi_k}{\partial x_\ell} \frac{\partial \phi_i'}{\partial x_j} dR + \int_R h_i \phi_i' dR \qquad (2.12)$$

By the same operations,

$$\int_C P_i' \phi_i dS = \int_R a_{ijk\ell} \frac{\partial \phi_k'}{\partial x_\ell} \frac{\partial \phi_i}{\partial x_j} dR + \int_R h_i' \phi_i dR \qquad (2.13)$$

We may now combine (2.12) and (2.13) to obtain the reciprocal relation

$$\int_C [P_i \phi_i' - P_i' \phi_i] dS = \int_R [h_i \phi_i' - h_i' \phi_i] dR \qquad (2.14)$$

since

$$a_{ijk\ell} \frac{\partial \phi_k}{\partial x_\ell} \frac{\partial \phi_i'}{\partial x_j} = a_{ijk\ell} \frac{\partial \phi_k'}{\partial x_\ell} \frac{\partial \phi_i}{\partial x_j} \qquad (2.15)$$

by the required symmetry condition (2.2).

2.1.4 A Fundamental Singular Solution

The heart of the BIE lies in finding a solution h_i in (2.10) which satisfies (2.1) at all points except $\underset{\sim}{x} = \underset{\sim}{x}_o$, ($\underset{\sim}{x}_o \in R$), whereby the singularity of the proposed solution yields the necessary information about $\phi_k(\underset{\sim}{x}_o)$

to make (2.14) an interior identity. In other words, we seek the solution to

$$a_{ijk\ell} \frac{\partial^2 \phi_k}{\partial x_j \partial x_\ell} = K_i \delta(\underset{\sim}{x} - \underset{\sim}{x}_o) \tag{2.16}$$

$$\underset{\sim}{x} = (x_1, x_2) \qquad \underset{\sim}{x}_o = (a,b)$$

where δ is the Dirac delta function and K_i are constants to be determined. A candidate for a solution would be the function ϕ_k of (2.9) with

$$f_\alpha(z_\alpha) = \frac{1}{2\pi i} D_\alpha \log(z_\alpha - c_\alpha) \tag{2.17}$$

where $c_\alpha \equiv a + p_\alpha b$ and D_α are constants. Accordingly, (2.9) becomes

$$\phi_k = \frac{1}{2\pi i} \{\sum_\alpha A_{k\alpha} D_\alpha \log(z_\alpha - c_\alpha) + \sum_\alpha \bar{A}_{k\alpha} \bar{D}_\alpha \log(\bar{z}_\alpha - \bar{c}_\alpha)\} \tag{2.18}$$

The multivalue properties of the logarithm provide that transversing any closed path encircling the point $\underset{\sim}{x}_o$ causes ϕ_k to jump by an amount

$$b_k = \sum_\alpha (A_{k\alpha} D_\alpha + \bar{A}_{k\alpha} \bar{D}_\alpha) \tag{2.19}$$

To make b_k identically zero, let

$$D_\alpha = \frac{1}{2} i \, N_{\alpha j} d_j \tag{2.20}$$

where d_j are real constants and

$$A_{k\alpha} N_{\alpha j} = \delta_{kj} \tag{2.21}$$

The existence of $N_{\alpha j}$ is guaranteed by the fact that $A_{k\alpha}$ is non-singular. The non-singular character of $A_{k\alpha}$ is established for the case when (2.8) has N distinct roots by an extension of a result obtained by Stroh [4] with N=3. By this choice of D_α, b_k is identically zero, making (2.18) a possible solution to (2.16).

This solution is valid everywhere with logarithmic singularity at $\underset{\sim}{x}_o$, which is admissible within the Dirac delta function. In order that (2.18) satisfy (2.16), we must relate the K_i to the D_α by the residue of the integral over an arbitrary region enclosing the point $\underset{\sim}{x}_o$.

We accomplish this by determining K_i directly from integration of (2.16) with ϕ_k as given by (2.18). By this substitution (2.16) becomes

$$\frac{1}{2\pi i}\left\{ a_{ilkl}\left[-\sum_\alpha \frac{A_{k\alpha}D_\alpha}{(z_\alpha-c_\alpha)^2} + \sum_\alpha \frac{\bar{A}_{k\alpha}\bar{D}_\alpha}{(\bar{z}_\alpha-\bar{c}_\alpha)^2}\right]\right.$$

$$+ a_{ilk2}\left[-\sum_\alpha \frac{A_{k\alpha}D_\alpha p_\alpha}{(z_\alpha-c_\alpha)^2} + \sum_\alpha \frac{\bar{A}_{k\alpha}\bar{D}_\alpha\bar{p}_\alpha}{(\bar{z}_\alpha-\bar{c}_\alpha)^2}\right]$$

$$+ a_{i2kl}\left[-\sum_\alpha \frac{A_{k\alpha}D_\alpha}{(z_\alpha-c_\alpha)^2} + \sum_\alpha \frac{\bar{A}_{k\alpha}\bar{D}_\alpha}{(\bar{z}_\alpha-\bar{c}_\alpha)^2}\right]$$

$$\left. + a_{i2k2}\left[-\sum_\alpha \frac{A_{k\alpha}D_\alpha p_\alpha}{(z_\alpha-c_\alpha)^2} + \sum_\alpha \frac{\bar{A}_{k\alpha}\bar{D}_\alpha\bar{p}_\alpha}{(\bar{z}_\alpha-\bar{c}_\alpha)^2}\right]\right\} \quad (2.22)$$

Define

$$L_{ij\alpha} \equiv (a_{ijkl} + p_\alpha a_{ijk2})A_{k\alpha} \quad (2.23)$$

From (2.7)

$$(a_{ilkl} + a_{ilk2}p_\alpha)A_{k\alpha} = -(a_{i2kl}p_\alpha + a_{i2k2}p_\alpha^2)A_{k\alpha}$$

Since $A_{k\alpha}$ is non-zero, it follows that

$$L_{il\alpha} = -p_\alpha L_{i2\alpha} \quad (2.24)$$

We can then write (2.22) as

$$\frac{1}{\pi i}\left(\sum_\alpha \frac{-L_{i2\alpha}D_\alpha p_\alpha}{(z_\alpha-c_\alpha)^2} + \sum_\alpha \frac{\bar{L}_{i2\alpha}\bar{D}_\alpha\bar{p}_\alpha}{(\bar{z}_\alpha-\bar{c}_\alpha)^2}\right) \quad (2.25)$$

Consideration of equation (2.16) shows that the only non-trivial information determined by the integration of (2.24) will be given by the point $\underset{\sim}{x}_o$. Therefore we can convert the region integral to an arbitrary contour integral surrounding $\underset{\sim}{x}_o$. For convenience we choose a square of sides of length two (with centroid c_α which we take as the origin) as our contour. Green's theorem yields the following

$$\int_R a_{ijk\ell} \frac{\partial^2 \phi_k}{\partial x_j \partial x_\ell} dx_1 dx_2$$

$$= \frac{1}{2\pi i} \int_C \left[\left(\sum_\alpha \frac{L_{i2\alpha} D_\alpha p_\alpha}{z_\alpha - c_\alpha} - \sum_\alpha \frac{\bar{L}_{i2\alpha} \bar{D}_\alpha \bar{p}_\alpha}{\bar{z}_\alpha - \bar{c}_\alpha} \right) dx_2 \right.$$

$$\left. + \left(\sum_\alpha \frac{L_{i2\alpha} D_\alpha}{z_\alpha - c_\alpha} \sum_\alpha \frac{\bar{L}_{i2\alpha} \bar{D}_\alpha}{\bar{z}_\alpha - \bar{c}_\alpha} dx_1 \right) \right] \qquad (2.26)$$

The result of (2.26) will be the following expression for our arbitrary constant K_i:

$$K_i = \sum_\alpha L_{i2\alpha} D_\alpha + \sum_\alpha \bar{L}_{i2\alpha} \bar{D}_\alpha \qquad (2.27)$$

or equivalently

$$K_i = -\frac{1}{2i} \sum_\alpha (L_{i2\alpha} N_{\alpha j} - \bar{L}_{i2\alpha} \bar{N}_{\alpha j}) d_j$$

Thus (2.18) is the sought solution if the D_α satisfy (2.20) and the K_i (2.27).

2.2 THE BOUNDARY INTEGRAL FORMULATION

2.2.1 General Formulation For Second Order Elliptic Systems

We may now use the fundamental singular solution and the reciprocal relation of section 2.1.3 to formulate the boundary integral equation. First we note that the solution which we found (2.16) is still arbitrary in K_i. If we let $K_i = \delta_{ij}F$, F an arbitrary constant, in (2.27) for j=1,2,...N, we introduce a dependence of ϕ_k on j. Denote this dependent variable Φ_{kj}, as it is obtained from (2.18), and denote the corresponding P_k obtained from (2.4) in its dependent form as Γ_{kj}. Consider the reciprocal relation (2.14). If we associate ϕ_i with Φ_{ij}, P_i' with Γ_{ij}, h_i' with $K_i\delta(\underset{\sim}{x}-\underset{\sim}{x}_o)$ and let the unprimed variables be a regular solution to (2.1) (i.e., $h_i=0$), we obtain

$$\int_C [P_i\phi_{ij} - \Gamma_{ij}\phi_i]ds = -F\int_R \phi_j\delta(\underset{\sim}{x}-\underset{\sim}{x}_o)dR \qquad (2.28)$$

We can realize an interior identity from (2.28) directly by familiar interpretations of the Dirac delta function. Alternatively we may realize it by the classical

fashion of deleting a square of sides 2ε surrounding the neighborhood of the singular point (Figure 1), and taking the limits (see Appendix I.1 for details). By either means, the interior identity is

$$\int_C [P_i(\underset{\sim}{X})\phi_{ij}(\underset{\sim}{X}, \underset{\sim}{x}_o) - \Gamma_{ij}(\underset{\sim}{X}, \underset{\sim}{x}_o)\phi_i(\underset{\sim}{X})]ds(\underset{\sim}{X})$$

$$= -\phi_j(\underset{\sim}{x}_o)F \qquad i,j = 1,2,\ldots N \qquad (2.29)$$

where upper case X denotes $\underset{\sim}{x} \in C$ and lower case c denotes $\underset{\sim}{x} \in R$.

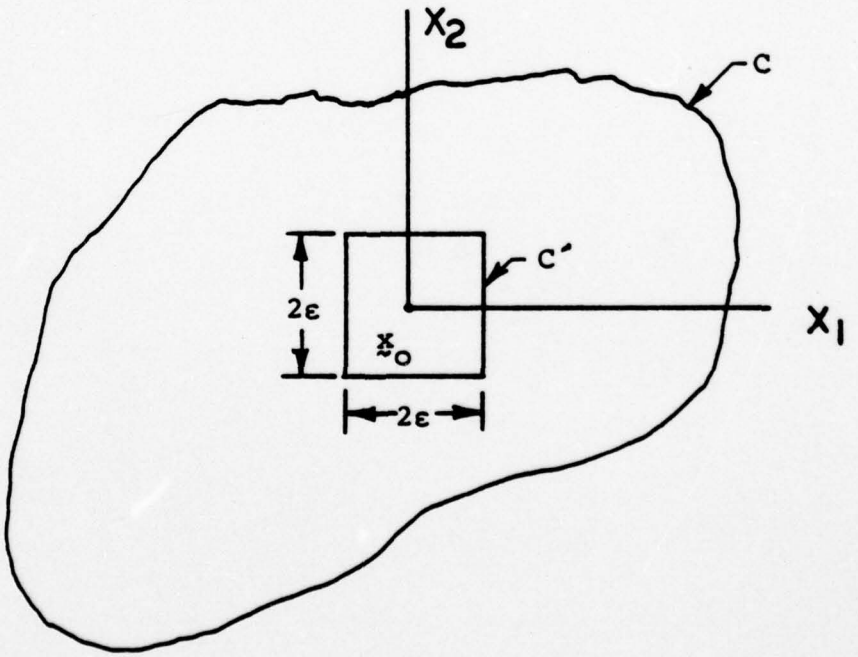

FIGURE 1

We now proceed to develop the boundary integral equation by letting $\underset{\sim}{x}_o$ become an element of C, which we will recognize $\underset{\sim}{x}_o$ by our notation convention as $\underset{\sim}{X}_o$. Augmenting the contour by a rectangle (Figure 2) to facilitate easier integration and taking the appropriate limits (see Appendix I.2) we arrive at the boundary integral equation

$$\int_C [P_i(\underset{\sim}{X})\Phi_{ij}(\underset{\sim}{X}, \underset{\sim}{X}_o) - \Gamma_{ij}(\underset{\sim}{X}, \underset{\sim}{X}_o)\phi_i(\underset{\sim}{X})]ds(\underset{\sim}{X})$$

$$= -\lambda_{ij}(\underset{\sim}{X}_o)F\phi_i(\underset{\sim}{X}_o) \qquad (2.30)$$

where λ_{ij} is related to the inner angle $\beta(\underset{\sim}{X}_o)$. By considering a uniform distribution of ϕ_i, which for convenience we take as unity, we may express $\lambda_{ij}(\underset{\sim}{X}_o)F$ as

$$\lambda_{ij}(\underset{\sim}{X}_o)F = \int_C \Gamma_{ij}(\underset{\sim}{X}, \underset{\sim}{X}_o)ds(\underset{\sim}{X}) \qquad (2.31)$$

Substituting (2.31) in (2.30) we have the boundary integral equation in its most general form

$$-\int_C \phi_i(\underset{\sim}{X}_o)\Gamma_{ij}(\underset{\sim}{X}, \underset{\sim}{X}_o)ds(\underset{\sim}{X})$$

$$= \int_C [P_i(\underset{\sim}{X})\Phi_{ij}(\underset{\sim}{X}, \underset{\sim}{X}_o) - \Gamma_{ij}(\underset{\sim}{X}, \underset{\sim}{X}_o)\phi_i(\underset{\sim}{X})]ds(\underset{\sim}{X})$$

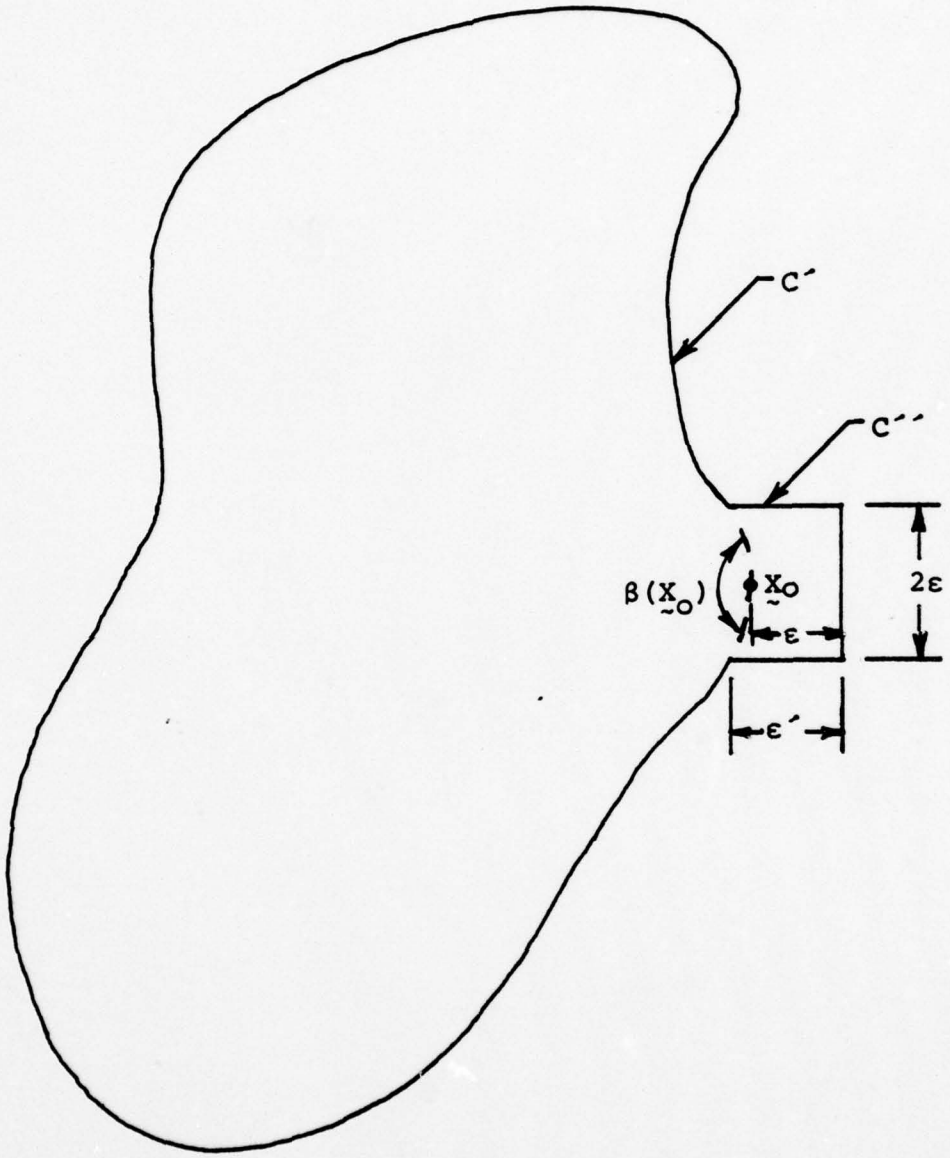

FIGURE 2

2.3 A NUMERICAL PROCEDURE

2.3.1 Numerical Implementation of The Boundary Integral Equation

We note forthright that (2.30) constitutes a singular integral equation from which an exact analytical solution could be determined in principle. However, this approach would be successful only for the most elementary problems. Moreover, in such cases the process would still require a tremendous effort as compared to other means of arriving at the same analytical solution. Therefore the BIE is applied by making a sufficient number of approximations to obtain a numerically realizable procedure. Specifically, the approach is to approximate the BIE by a system of linear algebraic equations that will be solved numerically to obtain the desired values of $\phi_i(\underset{\sim}{X})$ and/or $P_i(\underset{\sim}{X})$ according to the boundary value problem posed.

As a means to this end, four major steps are taken, all of which bear significantly on the final result. They can be categorized in occuring order as:

i) Discretization of the boundary;

ii) Boundary geometry representation;

iii) Boundary variable representation;

iv) Evaluation of integrals.

The discretization of the boundary is dividing of the boundary curve into m segments, C_σ, over which the BIE method is applied (Figure 3 depicts a typical

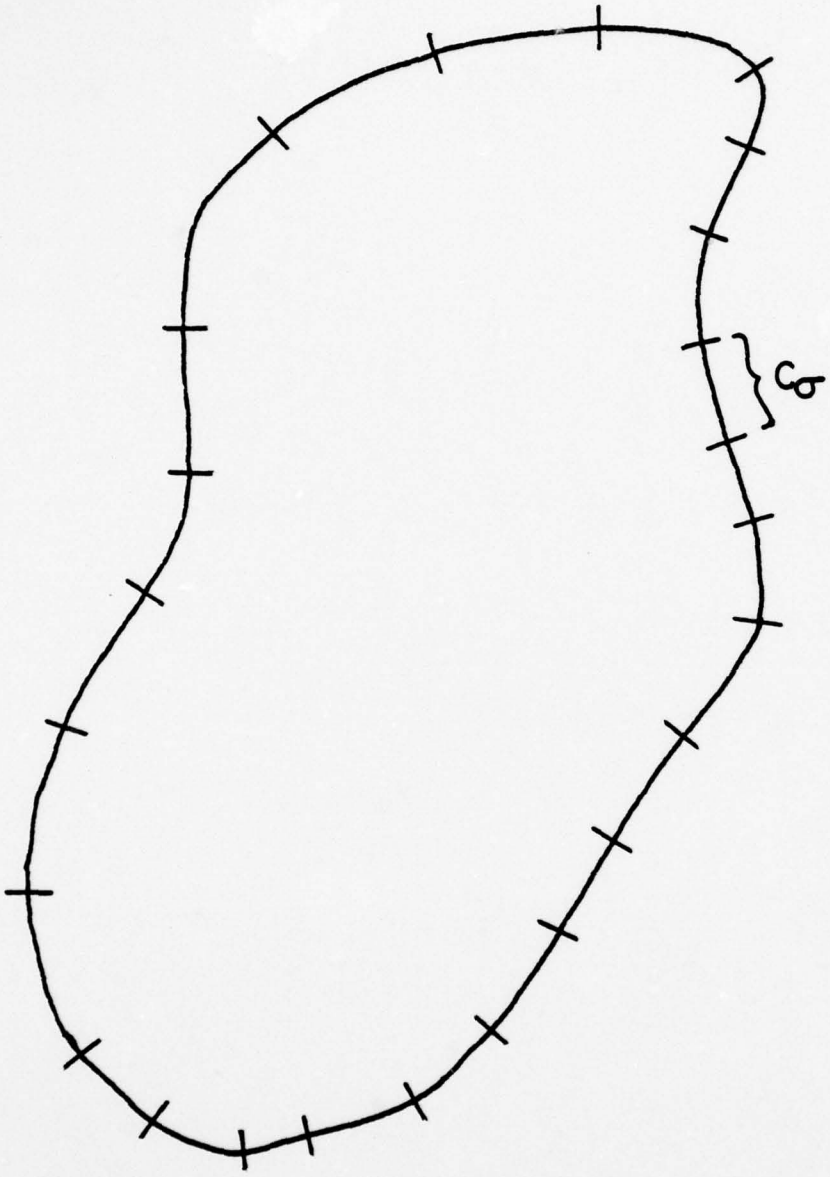

FIGURE 3

discretization pattern). The BIE (2.30) may then be written as

$$-\lambda_{ij}(\underset{\sim}{X}_o)F\phi_i(\underset{\sim}{X}_o) = \sum_{\sigma=1}^{m} \int_{C_\sigma} [P_i(\underset{\sim}{X})\Phi_{ij}(\underset{\sim}{X}, \underset{\sim}{X}_o) - \Gamma_{ij}(\underset{\sim}{X}, \underset{\sim}{X}_o)\phi_i(\underset{\sim}{X})]ds(\underset{\sim}{X}) \quad (2.32)$$

Although this step introduces no approximations, it has a very significant effect on the error which will arise from later approximations, as will be demonstrated. There is no mechanical procedure for this process, but descriptions of the other steps outline an "ad hoc" set of rules to follow in discretizing the boundary.

Usually, no approximations of boundary geometry need be made for two dimensional problems of interest; however, to establish a solution method which will numerically solve the generic problem, it will be found quite convenient to approximate the boundary geometry. Polynomial shape function approximations are the most straightforward approach, yet provide extremely good results using low order polynomials. Note that the error introduced here will depend heavily on the boundary discretization.

The representation of boundary variables is the first "true" approximation that need be made. We require it so that we may approximately replace the singular

integral equations involved with regular integral equations, in order that we obtain a simultaneous linear algebraic system in the boundary variables. Again, polynomial shape functions of a low order lend themselves to very good results in this approximation. Furthermore, considerations of the boundary variables should be made in conjunction with considerations of the boundary geometry when deciding upon a discretization pattern as we note that ϕ_i is a continuous function, whereas P_i is not necessarily continuous.

We now have a system of regular integral equations. At this point we have a choice regarding the manner in which we will evaluate these remaining integrals. We may evaluate them either analytically (employing the polynomial approximations made so far) or by numerical integration of a polynomial interpolating function. One can certainly appreciate the complexity of the integrals involved (which could very possibly lead to unobtainable analytical results) that is further increased by higher polynomial approximations of boundary variables, all of which make numerical integration more appealing. The choice of the numerical integration procedure must also be considered in the discretization process.

The execution of these steps allow us to arrive at a system of n simultaneous linear algebraic equations in n unknowns, which can be solved to obtain the desired boundary value data. The n referred to here is determined

by the number of segments (m) and the degree of the polynomial (γ) used to approximate the boundary variables.

2.3.2 Boundary Integral Equation Using Polynomial Shape Functions (PSFBIE)

Inherently the BIE requires integration along the contour (which we will approximate in practical problems of interest) that inevitably leads to difficulties in integration. Consequently, in the process of approximating boundary geometry and boundary variables there is a distinct advantage in changing the variable of integration by mapping each segment to a straight line.

This mapping is accomplished by expressing the cartesian coordinates of each point on the given segment in terms of the cartesian coordinates of the nodes and the coordinate ξ in the mapped space [1]. Similarly we express the boundary variables of each point in terms of the boundary variables of the nodes and the coordinate ξ in the mapped space. Mathematically we may express this as

$$\begin{aligned} X_j(Q) &= M^{\alpha}(\xi) X_j^{\alpha} \\ P_i(Q) &= M^{\alpha}(\xi) P_i^{\alpha} \qquad j = 1,2 \\ \phi_i(Q) &= M^{\alpha}(\xi) \phi_i^{\alpha} \qquad i = 1,2,\ldots N \end{aligned} \tag{2.33}$$

where Q is a point on the boundary where we are integrating, M^{α} is the polynomial of degree γ which is used to approximate the said variables, and α has the range of the number

of nodes on the segment $(\gamma + 1)$. Figure 4 shows a graphical interpretation of the first relation of (2.33). The coefficients of the polynomials M^{α} depend upon the locations of the nodes in the mapped space. Logically, we would locate the nodes symmetrically on the straight line in the mapped space. Furthermore, we will define $\xi=0$ as the midpoint of the straight line.

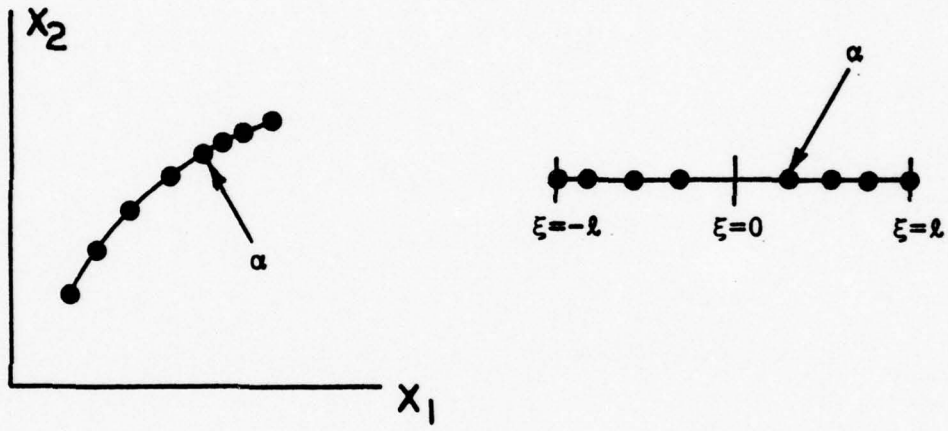

FIGURE 4

The mapping procedure outlined so far has an associated Jacobian which is used in the evaluation of integrals in the real space. In other words, $ds(\underset{\sim}{X})$ must be expressed as $J(\xi)d\xi$. To obtain $J(\xi)$ consider the differential elements depicted in Figure 5 which are related as

$$ds^2 = dX_1^2 + dX_2^2 \qquad (2.34)$$

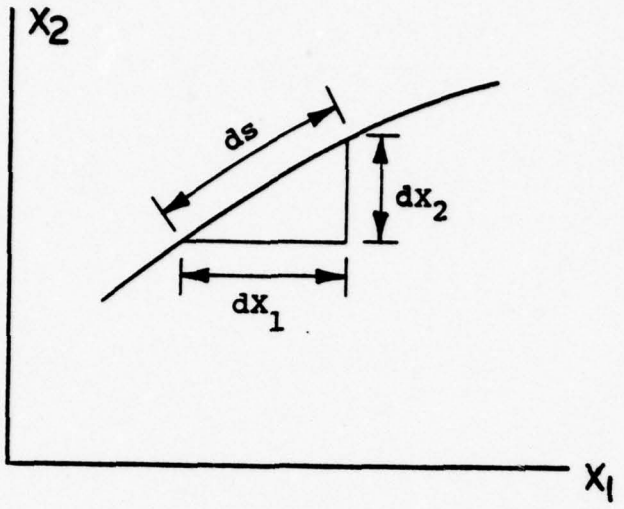

FIGURE 5

Using (2.33), the differential dX_j is

$$dX_j = \frac{dM^{\alpha}(\xi)}{d\xi} d\xi X_j^{\alpha} \tag{2.35}$$

for which the case of j=1,2 yields

$$ds = \sqrt{\left(\frac{dM^{\alpha}(\xi)}{d\xi} x_1^{\alpha}\right)^2 + \left(\frac{dM^{\alpha}(\xi)}{d\xi} x_2^{\alpha}\right)^2} d\xi$$

$$= J(\xi)d\xi \tag{2.36}$$

Equation (2.32) may now be expressed as

$$-\lambda_{ij}(\underset{\sim}{X}_o) F\phi_i(\underset{\sim}{X}_o) = \sum_{\sigma=1}^{m} \int_{C_\sigma} \{M^{\alpha}(\xi)[P_i^{\alpha\sigma}\Phi_{ij}(\underset{\sim}{X}(\xi), \underset{\sim}{X}_o)$$

$$- \Gamma_{ij}(\underset{\sim}{X}(\xi), \underset{\sim}{X}_o)\phi_i^{\alpha\sigma}]\}J(\xi)d\xi \tag{2.37}$$

where $P_i^{\alpha\sigma}$ is interpreted as the i component of P on segment σ at local node α and $\phi_i^{\alpha\sigma}$ has a similar interpretation.

2.3.3 Numerical Quadrature of Integrals in the PSFBIE

A broad definition of numerical quadrature may be taken as the numerical integration of a polynomial interpolating function, which will yield an exact result if the function to be integrated is of the same order as the interpolating function or less. Mathematically, this can be expressed as

$$\int_{\Delta\xi} f(\xi)d\xi \doteq [\sum_{i=1}^{\nu} w_i f(\xi_i)]\Delta\xi \qquad (2.38)$$

where $\Delta\xi$ is the interval over which we are integrating, ν is the number of function evaluations in $\Delta\xi$, and ξ_i are the roots of the interpolating function (in the interval in which it is valid) with appropriate weights w_i.

For quadrature formulae of the form (2.38) the most accurate are Gaussian quadrature formulas [5]. The particular type of Gaussian quadrature is determined by the interpolating polynomial associated with it. As yet, the length of the straight line in section 2.3.3 purposely has not been specified with the foresight of choosing it to obtain the most accurate numerical quadrature in the mapped space. Accordingly, the choice of Legendre-Gauss

Quadrature determines the straight line as the interval $\xi=-1$ to $\xi=1$. This choice leads to the exact integration of polynomials of degree $2\nu-1$ or less where ν is the number of function evaluations in (2.38).

Note that (2.35) contains singular integrals when $\underset{\sim}{X}_o$ is on segment σ. In this case Legendre-Gauss Quadrature will not give accurate results. Consequently, modifications must be made, for which the reader is referred to Appendix II. Appendix II also describes the evaluation of non-singular integrals involved in the calculation of the coefficient matrix.

2.3.4 Assembly and Solution of the Coefficient Matrix

We now seek to represent the Boundary Integral Equation in its present form (2.37) as a matrix equation so that we may solve it as a simultaneous linear algebraic system. Note that by using (2.31), equation (2.30) can be expressed as

$$\int_C [\phi_i(\underset{\sim}{X}) - \phi_i(\underset{\sim}{X}_o)]\Gamma_{ij}(\underset{\sim}{X}, \underset{\sim}{X}_o)ds(\underset{\sim}{X})$$

$$= \int_C P_i(\underset{\sim}{X})\Phi_{ij}(\underset{\sim}{X}, \underset{\sim}{X}_o)ds(\underset{\sim}{X}) \qquad (2.39)$$

whereby its counterpart in the PSFBIE equation (2.37) assumes the form

$$\sum_{\sigma=1}^{m}\left\{\int_{C_\sigma}\phi_i^{\alpha\sigma}M^\alpha(\xi)\Gamma_{ij}(\underset{\sim}{X}(\xi),\ \underset{\sim}{X}_o)J(\xi)d\xi\right.$$

$$\left.-\ \phi_i(\underset{\sim}{X}_o)\int_{C_\sigma}\Gamma_{ij}(\underset{\sim}{X}(\xi),\ \underset{\sim}{X}_o)J(\xi)d\xi\right\}$$

$$=\sum_{\sigma=1}^{m}\int_{C_\sigma}P_i^{\alpha\sigma}M^\alpha(\xi)\Phi_{ij}(\underset{\sim}{X}(\xi),\ \underset{\sim}{X}_o)J(\xi)d\xi \qquad (2.40)$$

When calculating the indicated integrals (either analytically or numerically), equation (2.40) can be concisely formulated in matrix form as

$$\sum_{\sigma=1}^{m}[\phi_i^{\alpha\sigma}a_{ij}^{\alpha\sigma}-\phi_i(\underset{\sim}{X}_o)F\lambda_{ij}^{\sigma}]=\sum_{\sigma=1}^{m}P_i^{\alpha\sigma}b_{ij}^{\alpha\sigma} \qquad (2.41)$$

or

$$[A]\{\phi\}=[B]\{P\} \qquad (2.42)$$

where $[A]=[a_{ij}^{\alpha\sigma}-F\lambda_{ij}^{\sigma}]$

$\{\phi\}=\{\phi_i^{\alpha\sigma}\}$

$[B]=[b_{ij}^{\alpha\sigma}]$

$\{P\}=\{P_i^{\alpha\sigma}\}$

$$a_{ij}^{\alpha\sigma} = \int_{C_\sigma} M^\alpha(\xi)\Gamma_{ij}(\underset{\sim}{X}(\xi), \underset{\sim}{X}_o)J(\xi)d\xi \tag{2.43}$$

$$F\lambda_{ij}^{\sigma} = \int_{C_\sigma} \Gamma_{ij}(\underset{\sim}{X}(\xi), \underset{\sim}{X}_o)J(\xi)d\xi \tag{2.44}$$

$$b_{ij}^{\alpha\sigma} = \int_{C_\sigma} M^\alpha(\xi)\Phi_{ij}(\underset{\sim}{X}(\xi), \underset{\sim}{X}_o)J(\xi)d\xi \tag{2.45}$$

The details of the calculation of $a_{ij}^{\alpha\sigma}$, $\lambda_{ij}^{\alpha\sigma}$ and $b_{ij}^{\alpha\sigma}$ for both singular (i.e., $\underset{\sim}{X}_o$ on segment σ) and non-singular integrals evaluated numerically are supplied in Appendix II. The elliptic system (2.1) will then be solved according to the form of the boundary conditions.

For the Dirchlet problem, (2.42) becomes

$$\{c\} = [B]\{P\} \tag{2.46}$$

where $\{c\} = [A]\{\phi\}$.

For the Neuman problem we have

$$[A]\{\phi\} = \{c\} \tag{2.47}$$

where $\{c\} = [B]\{P\}$. However, Neuman problems do not have unique solutions, making the [A] matrix singular. To deal with this situation, we constrain one value of $\{\phi_i^{\alpha\sigma}\}$ arbitrarily, so that we may uniquely obtain all other values of $\{\phi_i^{\alpha\sigma}\}$. This could be realized by specifying one $\{\phi_i^{\alpha\sigma}\}$ to be zero and then eliminating

the corresponding row and column in [A] and the corresponding element of {c}. Thus we deal with the reduced system.

$$[A^*]\{\phi^*\} = \{c^*\} \tag{2.48}$$

Altneratively, the value of one element of $\{\phi_i^{\alpha\sigma}\}$ may be specified arbitrarily and, considering the corresponding $\{P_i^{\alpha\sigma}\}$ to be unknown, the system can be solved as a mixed problem as will be outlined next.

For a mixed problem, (2.42) can be expressed as

$$[A^*]\{\phi^*\} = \{c^*\} \tag{2.49}$$

where $[A^*] = [a_{ij}^{\alpha^*}]$

$\{\phi^*\} = \{\phi_i^{\alpha\sigma^*}\}$ $\qquad 1 \leq i,j \leq N$

$\{c^*\} = [B^*]\{P^*\} = [b_{ij}^{\alpha\sigma^*}]\{P_i^{\alpha\sigma^*}\}$

The starred quantities are defined per the known boundary variables on segment σ. For a segment where ϕ_i is defined

$$\begin{aligned} a_{ij}^{\alpha\sigma^*} &= b_{ij}^{\alpha\sigma} \\ b_{ij}^{\alpha\sigma^*} &= a_{ij}^{\alpha\sigma} \\ \phi_i^{\alpha\sigma^*} &= P_i^{\alpha\sigma} \\ P_i^{\alpha\sigma^*} &= \phi_i^{\alpha\sigma} \end{aligned}$$

and for a segment where P_i is defined

$$
\begin{aligned}
a_{ij}^{\alpha\sigma *} &= a_{ij}^{\alpha\sigma} \\
b_{ij}^{\alpha\sigma *} &= b_{ij}^{\alpha\sigma} \\
\phi_i^{\alpha\sigma *} &= \phi_i^{\alpha\sigma} \\
p_i^{\alpha\sigma *} &= p_i^{\alpha\sigma}
\end{aligned}
$$

The previously unknown boundary data in equation (2.46), (2.48) or (2.49) may now be solved for by any of various standard methods.

Once the unknown boundary data is obtained by one of these means, the $\phi_j(\underset{\sim}{X}_o)$ in the interior identity (2.29) may be evaluated directly from a polynomial shape function adaptation of (2.29).

CHAPTER THREE

TEST PROBLEMS

3.1 PLANE ANISOTROPIC HEAT CONDUCTION

3.1.1 Application of Boundary Integral Equation Formulation

For the problem of plane anisotropic heat conduction the governing differential equation (2.1) takes the form

$$a_{j\ell} \frac{\partial \phi}{\partial x_j \partial x_\ell} = 0 \qquad j,\ell = 1,2 \qquad (3.1)$$

where our symmetry requirement (2.2) provides that $a_{j\ell}=a_{\ell j}$. The characteristic parameter P_α may be solved from (2.8) as

$$p_\alpha = \frac{-a_{12} \pm \sqrt{a_{12}^2 - a_{11}a_{22}}}{a_{22}} \qquad (3.2)$$

The determination of A from (2.7) is now arbitrary, which we choose as unity for convenience. It then follows that N is also unity by (2.21). The L of (2.23) are then

$$L_j = (a_{j1} + p_\alpha a_{j2}) \qquad (3.3)$$

The only L_j of significance is L_2, which is used for the determination of d in terms of K, viz.

$$d = \frac{-2K}{a_{22}i(p_\alpha - \bar{p}_\alpha)} \tag{3.4}$$

Finally D is determined from (2.20) as

$$D = \frac{-K}{a_{22}(p_\alpha - \bar{p}_\alpha)} \tag{3.5}$$

and the fundamental solution is assembled per equation (2.18). Now K is taken as unity per section 2.2.1 and ϕ becomes associated with Φ, while

$$\Gamma = a_{j\ell} \frac{\partial \phi}{\partial x_\ell} n_j \tag{3.6}$$

to arrive at the boundary integral equation.

3.1.2 Solved Problems

The purpose of this section is twofold. First and foremost, it is to demonstrate the ability of the method to solve problems of physical significance reliably and secondly to show the limited amount of input required in both data preparation and actual computer input. To accomplish this, two problems are solved: one for which the exact solution is known, where the comparison can be made directly; and the other one which by its nature allows us to draw on our intuition to assess the reliability of the solution. Furthermore, essential parameters of the particular problems are varied to demonstrate the ability of the method to discern the

variation.

(a) Consider a linear temperature distribution, $\phi=cx_1+d$, across a rectangular region of dimensions 2ℓ x $2w$ as shown in Figure 6. Now P can be expressed as

$$P = a_{11}cn_1 + a_{12}cn_2$$

Since we have analytical expressions for both temperature and heat flux as functions of position, we will consider the problem as a mixed one.

The nature of this problem also lends itself to be used to demonstrate another important aspect of the solution procedure which heretofore has received little attention, namely the accuracy of the method as the system becomes weakly elliptic. The weakening of the ellipticity is apparent from equation (3.2) as the discriminant approaches zero. Thus the approach is strictly a function of the material parameters $a_{j\ell}$.

In order that we may follow this approach analytically, we set a_{11} to unity, a_{12} to zero, leave a_{22} as a variable and rotate the material through an arbitrary angle θ. The transformed material parameters are given generally as

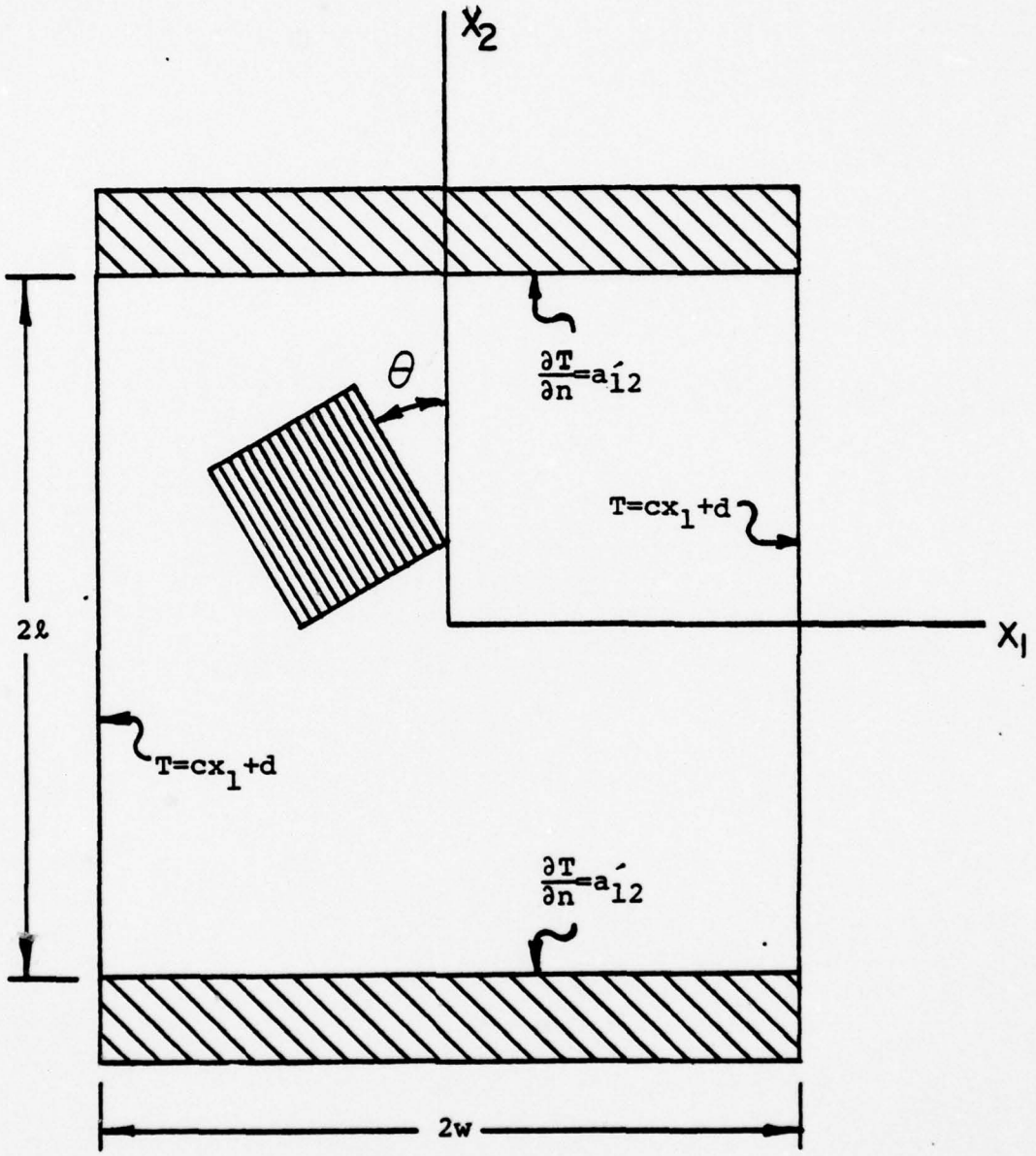

FIGURE 6

$$\begin{Bmatrix} a'_{11} \\ a'_{22} \\ a'_{12} \end{Bmatrix} = \begin{bmatrix} \cos^2\theta & \sin^2\theta & 2\sin\theta\cos\theta \\ \sin^2\theta & \cos^2\theta & -2\sin\theta\cos\theta \\ -\sin\theta\cos\theta & \sin\theta\cos\theta & (\cos^2\theta-\sin^2\theta) \end{bmatrix} \begin{Bmatrix} a_{11} \\ a_{22} \\ a_{12} \end{Bmatrix} \quad (3.7)$$

Investigating $da'_{12}/d\theta$ to find θ such that a'_{12} is a maximum, which would cause the system to become parabolic, we find

$$\frac{da'_{12}}{d\theta} = 0 = \sin^2\theta - \cos^2\theta + a_{22}(\cos^2\theta-\sin^2\theta)$$

which leads to

$$\cos^2\theta = 1/2$$

indicating that the maximum occurs at $\theta=\pi/4$. Substituting this value into (3.7) leads to

$$a'_{11} = (a_{22} + 1)/2$$

$$a'_{22} = (a_{22} + 1)/2$$

$$a'_{12} = (a_{22} - 1)/2$$

so that in the limit as a_{22} approaches infinity all of the transformed parameters become equal, thus indicating a parabolic system.

We arbitrarily set dimensions ℓ and w to unity and

take the constants of the exact solution ϕ, c and d, also to be unity while a_{22} is varied for $\theta=\pi/4$. The small amount of input required can be seen by using the crudest possible discretization for a quadratic shape function BIE (QSFBIE) of one segment per side for a total of eight nodes.

The problem is posed with temperature specified on $x_1 = \pm\ell$ and flux specified on $x_2 = \pm w$, for which boundary solution comparisons are summarized in Table 1 and depicted graphically in Figure 7. All solutions were obtained using a 4-point Legendre Gauss rule for numerical quadrature. The average absolute error (ϵ_Ψ) of Table 1 is defined as

$$\epsilon_\Psi = \frac{1}{M_\Psi} \frac{\sqrt{(\Psi_{BIE} - \Psi_{exact})^2}}{\Psi_{exact}} \qquad (3.8)$$

where Ψ is either variable being solved for in the mixed problem (T or $\partial T/\partial n$) and M_Ψ is the number of nodes at which the particular variable is solved for.

(b) Consider the problem of a rectangular region subject to uniform temperatures at two opposing sides and insulated on the other two sides as depicted in Figure 8. The problem is a mixed type for which there is no known analytical solution. However, in the general case of plane anisotropic heat conduction, the specifics of the problem allow a limited analysis which provides a "check" of sorts on the solution.

TABLE 1

AVERAGE ABSOLUTE ERRORS x 10^4

$\theta = \pi/4$

$\frac{a_{22}}{a_{11}}$	DISCRIMINANT	FLUXES	TEMPERATURES
2	2.	12	2
3	3.	16	2
4	4.	18	7
5	5.	24	8
6	6.	28	3
7	7.	33	7
8	8.	52	24
9	9.	73	47
10	10.	93	76
11	11.	114	109
12	12.	113	147
13	13.	174	188
14	14.	176	234
15	15.	196	282

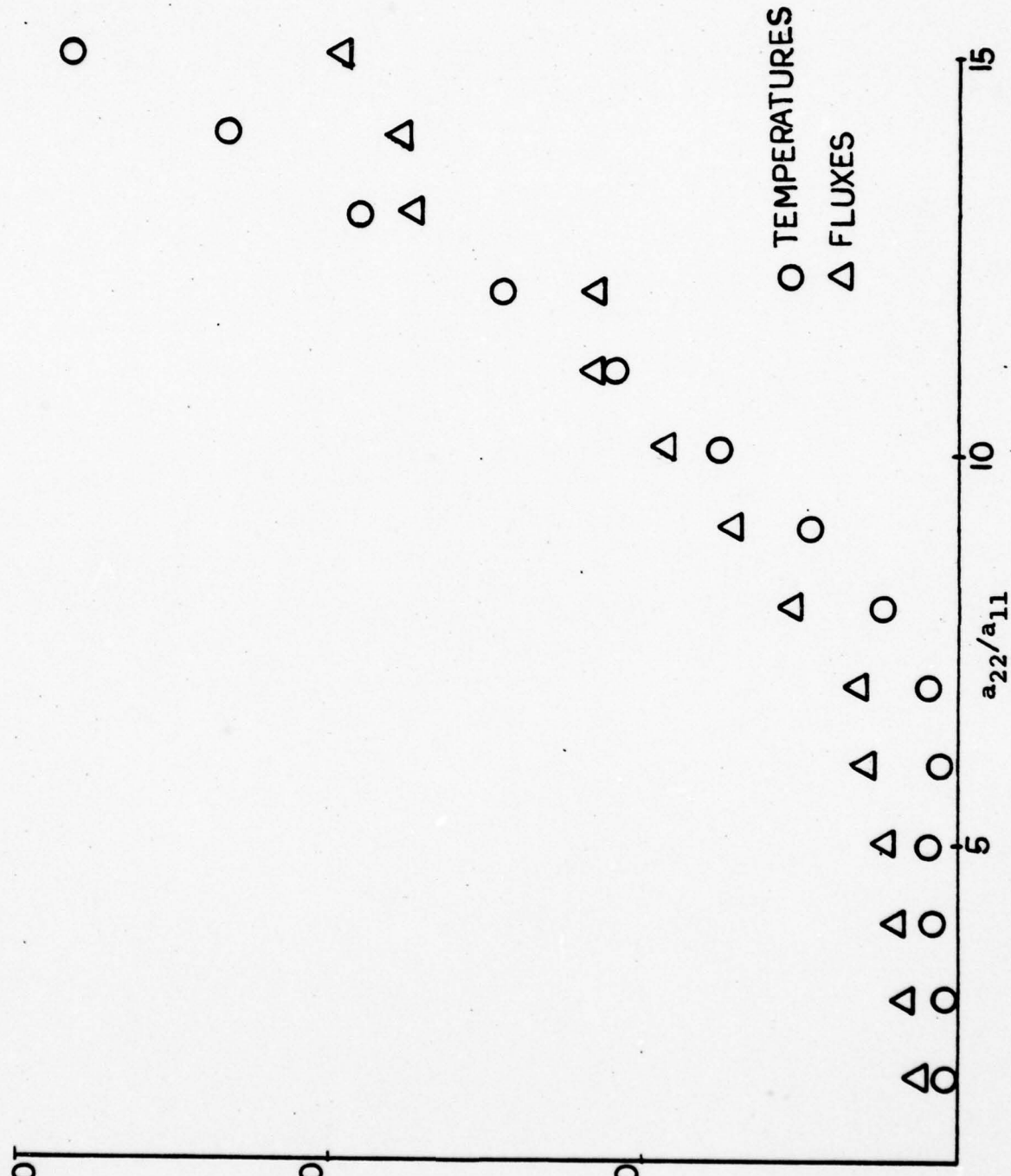
AVERAGE ABSOLUTE ERROR ϵ_y [PERCENT]
3.0
2.0
1.0
5
10
15
a_{22}/a_{11}
O TEMPERATURES
Δ FLUXES

FIGURE 7

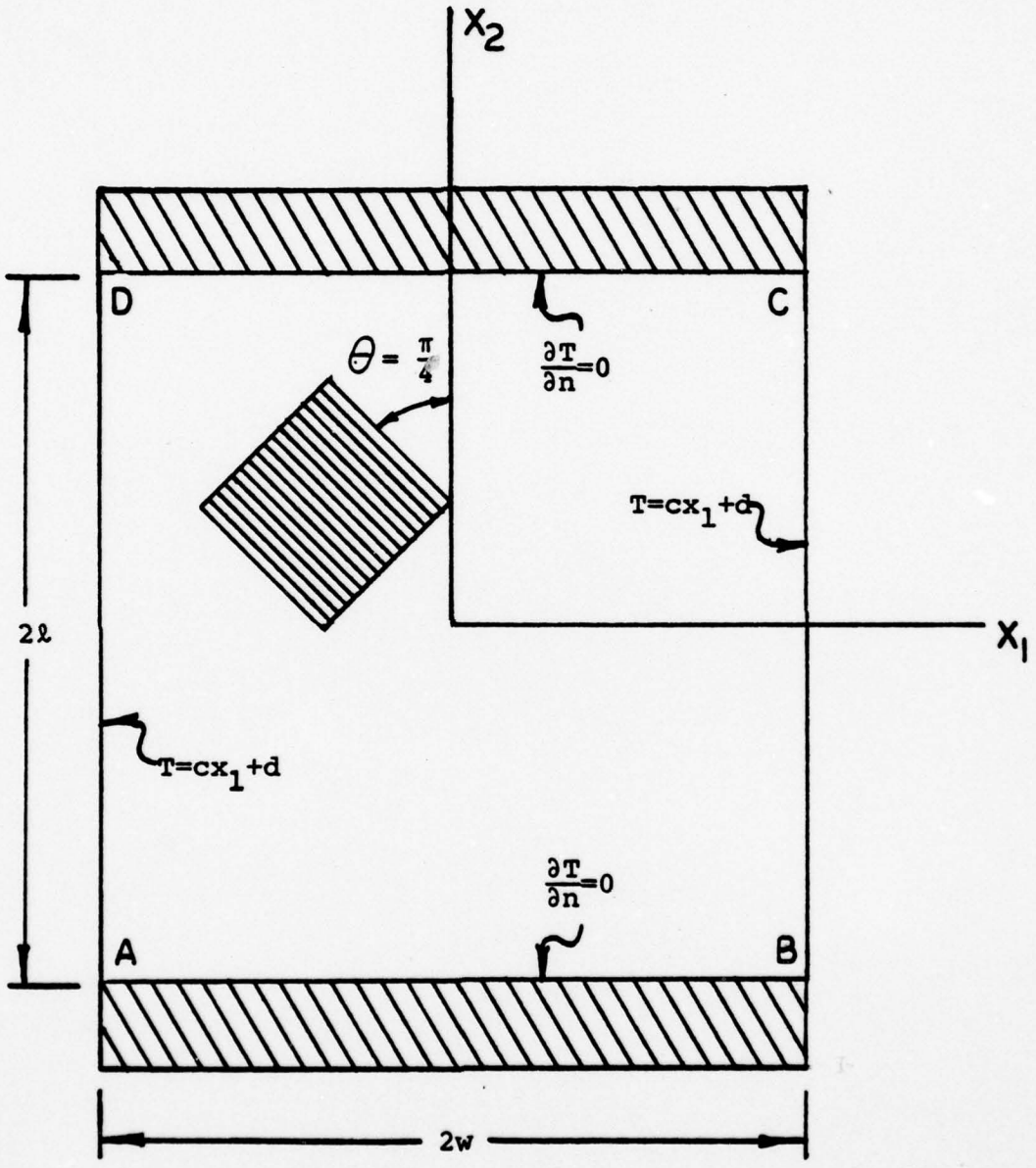
X_2
D
C
$\theta = \frac{\pi}{4}$
$\frac{\partial T}{\partial n}=0$
$T=cx_1+d$
2ℓ
X_1
$T=cx_1+d$
$\frac{\partial T}{\partial n}=0$
A
B
2w

FIGURE 8

Consider the intersection of an isotherm with an arbitrary contour as shown in Figure 9. If we define the intrinsic coordinate s along the isotherm, the chain rule for differentiation can be used to express the direction of the variation of T with s as

$$\frac{\partial T}{\partial s} = \frac{\partial T}{\partial x_1}\frac{\partial x_1}{\partial s} + \frac{\partial T}{\partial x}\frac{\partial x_2}{\partial s} \qquad (3.9)$$

where the position vector $\underset{\sim}{x}(s)$ of an arbitrary point (Q) with respect to the origin is given by

$$\underset{\sim}{x}(s) = x_1(s)\underset{\sim}{e}_1 + x_2(s)\underset{\sim}{e}_2 \qquad (3.10)$$

and $\underset{\sim}{e}_j$ is a unit vector basis defined in the direction of the coordinates x_j. Along an isotherm $\partial T/\partial s$ is

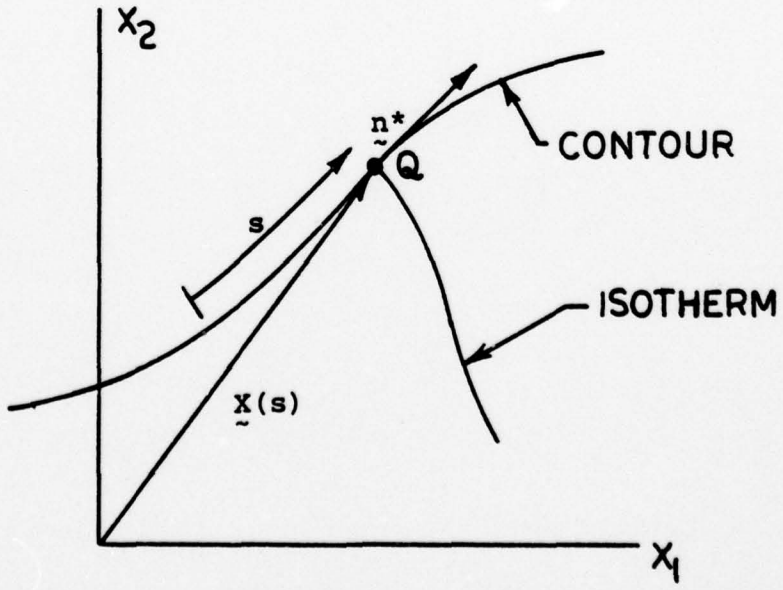

FIGURE 9

necessarily zero and $\partial x_j/\partial s$ will be a unit vector tangent to the isotherm which we will denote n_j^*. Thus equation (3.9) yields

$$\frac{\partial T}{\partial x_1} n_j^* = \frac{-\partial T}{\partial x_2} n_j^* \qquad j = 1,2 \qquad (3.11)$$

The definition of an isotherm provides that it is a line of constant flux, the value of which can be expressed on the boundary as

$$a_{j\ell} \frac{\partial T}{\partial x_\ell} n_j = k \qquad (3.12)$$

where k is a constant and n_j are components of the outward normal of the boundary. Now we satisfy equation (3.11) in order to use the relation (3.12). Choosing

$$n_1^* = \frac{\partial T}{\partial x_2} \qquad n_2^* = \frac{-\partial T}{\partial x_1} \qquad (3.13)$$

equation (3.11) is satisfied identically and can be used to determine the direction in which the isotherms intersect the boundary C.

We apply this analysis to the problem in question by noting that the two opposing sides maintained at uniform temperatures will have $\underset{\sim}{n}^*$ parallel to the outward normal of the boundary while along the insulated sides, k in equation (3.12) is zero. Because k is zero, we may express

equation (3.12) along sides AB and CD as

$$a_{21} \frac{\partial T}{\partial x_1} + a_{22} \frac{\partial T}{\partial x_2} = 0 \tag{3.14}$$

Using equation (3.13) we obtain

$$-a_{21}n_2^* + a_{22}n_1^* = 0 \tag{3.15}$$

which we satisfy by choosing

$$n_1^* = a_{21} \qquad n_2^* = a_{22} \tag{3.16}$$

so that the direction of the directional derivative (3.9) is given by equation (3.16). Note that the direction $\underset{\sim}{n}^*$ is the same along AB and CD.

To demonstrate the ability of the method to recognize variations in parameters, the problem is posed similar to problem (a) (i.e., $a_{11}=1$, $a_{12}=0$, $a_{22}=a_{22}$, $\ell=w=1$) except that this time a_{22}/a_{11} is fixed and θ is varied so that equations (3.16) can be expressed as

$$\begin{aligned} n_1^* &= a'_{21} = (a_{22} - a_{21})\cos\theta\sin\theta \\ n_2^* &= a'_{22} = a_{22}\cos^2\theta + a_{11}\sin^2\theta \end{aligned} \tag{3.17}$$

The stability of the solution procedure is demonstrated by choosing a_{22} as 10 (representing a highly anisotropic material). Note that this problem as posed reduces to problem (a) if $\theta=m\pi/2$. This check can be realized only approximately by a numerical procedure; however, the fact that $\underset{\sim}{n}^*$ is the same for a given isotherm along AB and CD can be seen from the graphical interpretation of the results (Figures 10-19).

Figures 10-14 are temperature contour maps of a 40 node boundary solution and subsequent interior point evaluations (a 9x9 square gridwork of points within the geometry of the problem). Continuity of contours was obtained by linear interpolation of the above data points in both the x_1 and the x_2 directions. The values marked within the different regions designate the temperature ranges given in Table 2.

Figures 15-19 are isometric plots of temperature versus position viewed from four different azimuths (ψ) for clearer interpretation. Nodes of the gridwork represent uniformly spaced points at which the temperature was evaluated numerically (with the exception of lines AD and BC, where the temperature was specified). Nodes along lines AB and CD are boundary solution points and all other nodal temperatures were evaluated subsequently by the interior identity by using the boundary solution.

TABLE 2

LEGEND FOR FIGURES 10-14

VALUE	TEMPERATURE RANGE
0	0.00-0.15
1	0.15-0.35
2	0.35-0.55
3	0.55-0.75
4	0.75-0.95
5	0.95-1.15
6	1.15-1.35
7	1.35-1.55
8	1.55-1.75
9	1.75-1.95
10	1.95-2.00

$$\theta = \frac{\pi}{12}$$

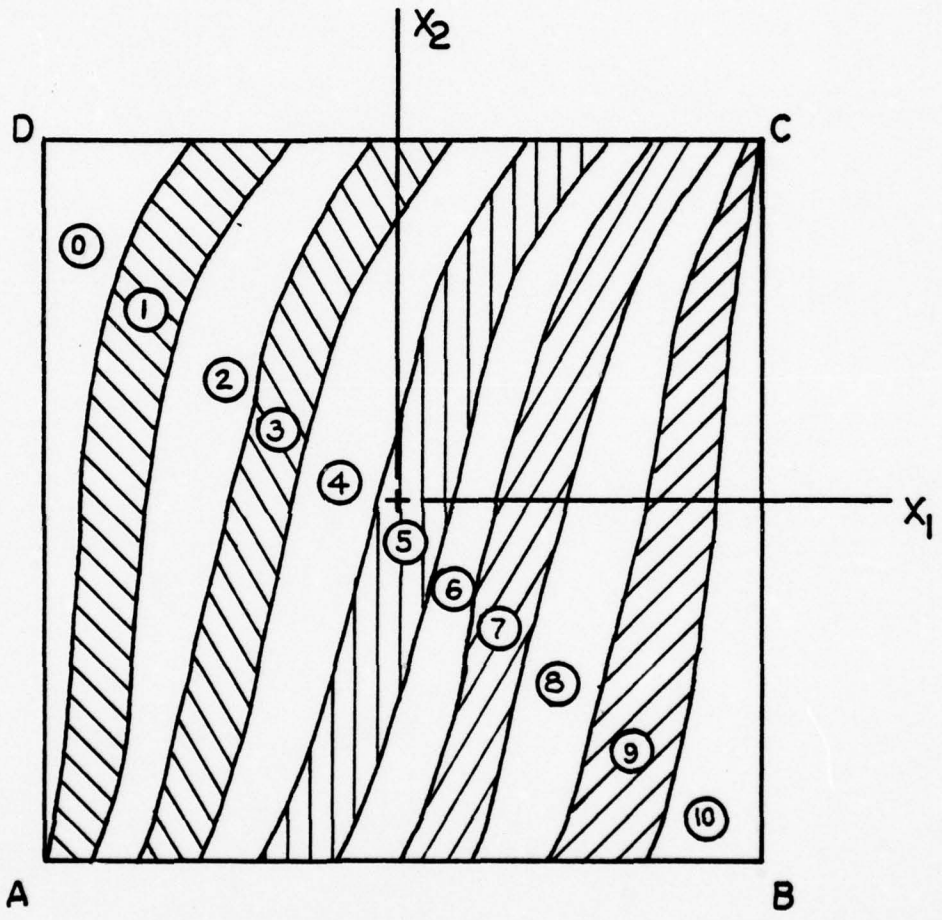

FIGURE 10

$$\theta = \frac{\pi}{6}$$

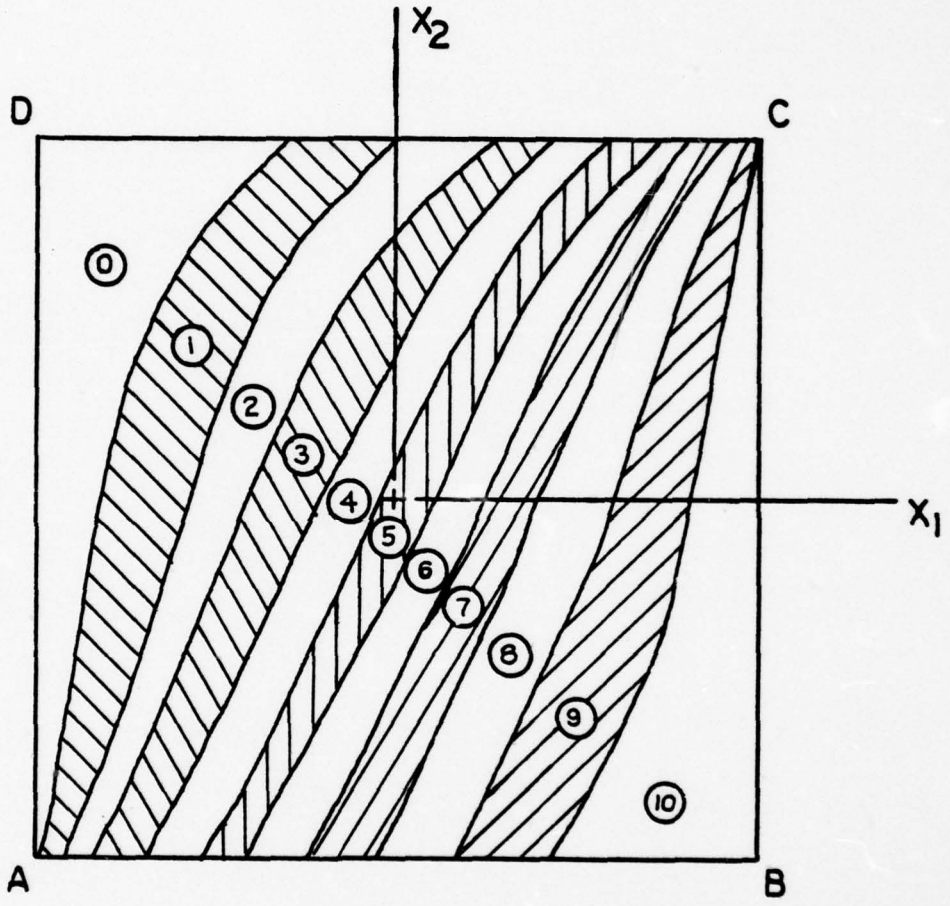

FIGURE 11

$$\theta = \frac{\pi}{4}$$

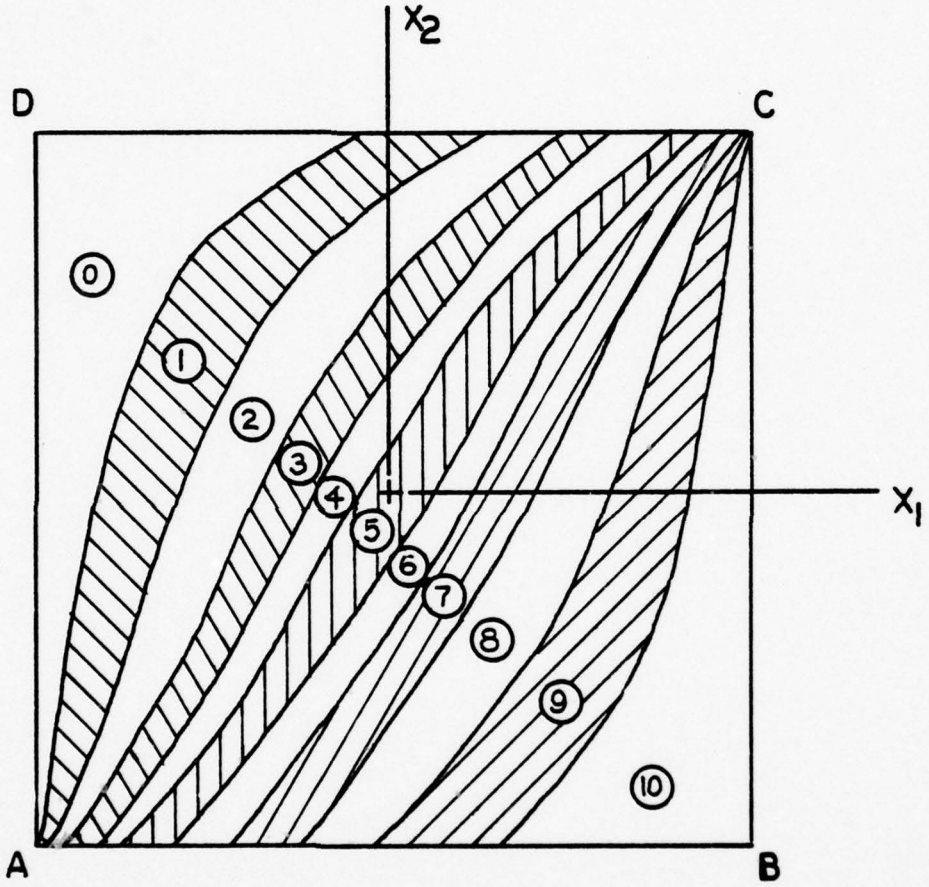

FIGURE 12

$$\theta = \frac{\pi}{3}$$

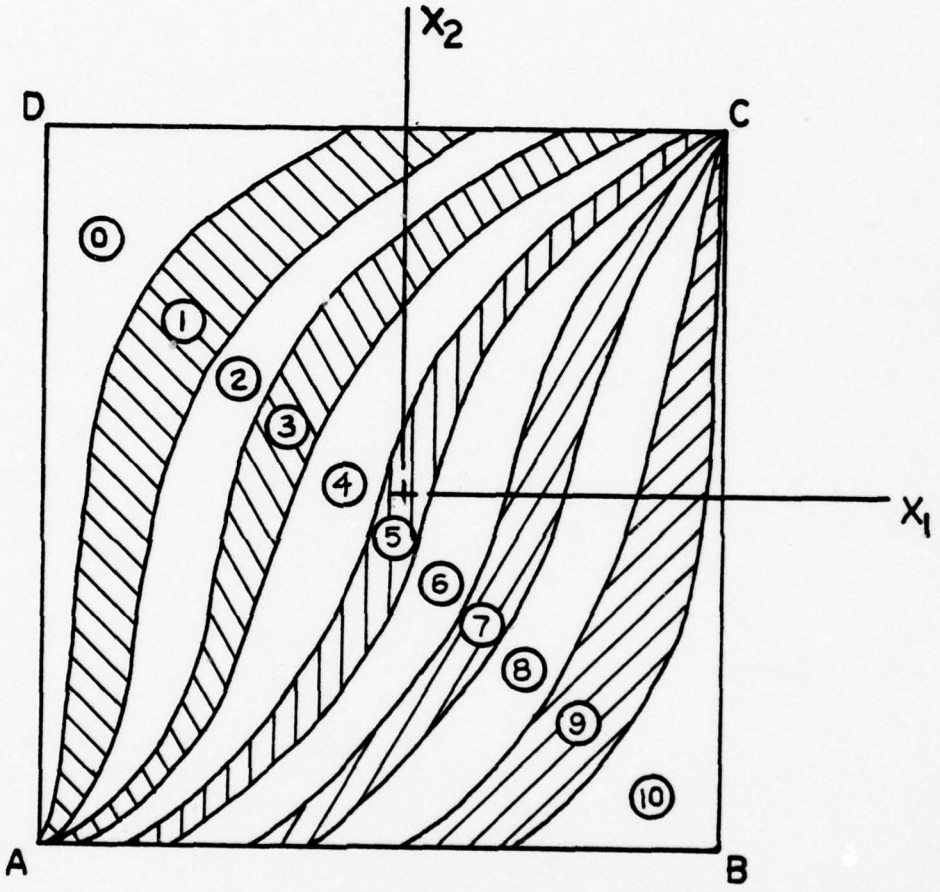

FIGURE 13

$$\theta = \frac{5\pi}{12}$$

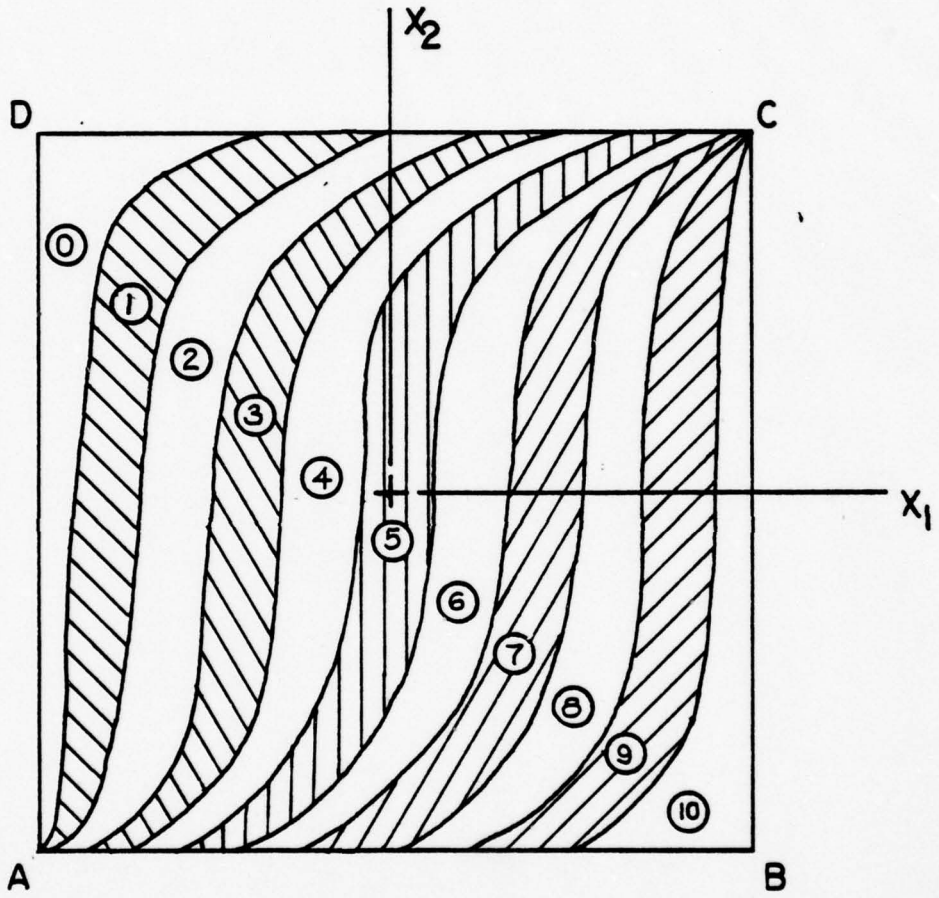

FIGURE 14

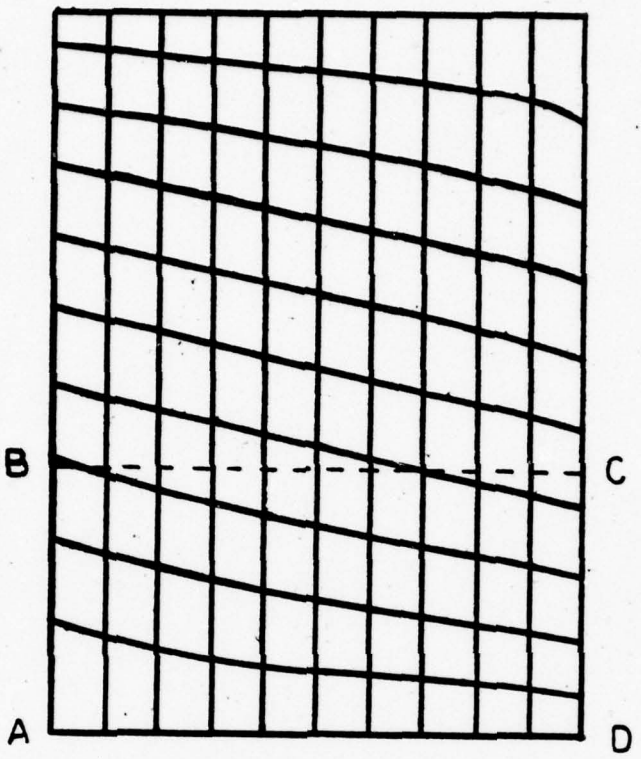

$\theta = \frac{\pi}{12}$

$\psi = 0$

FIGURE 15a

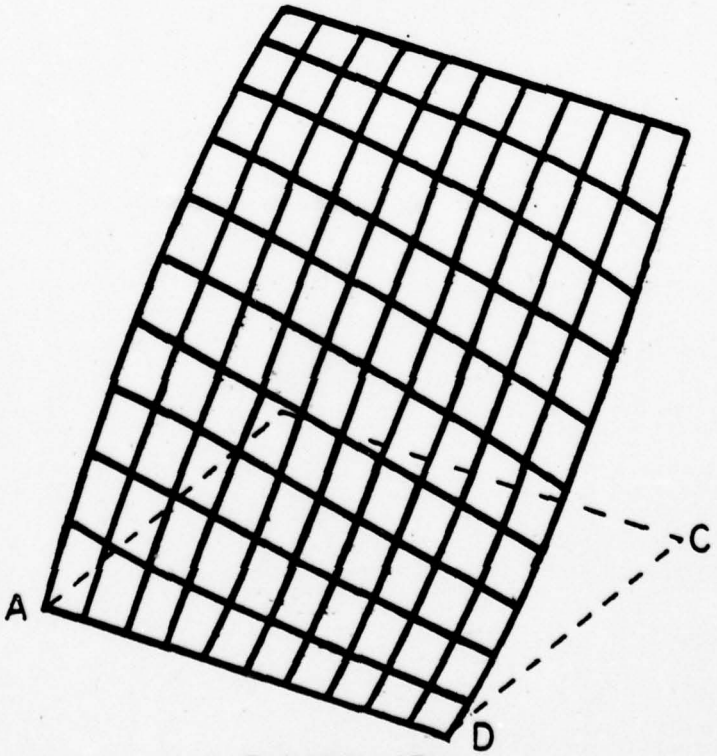

$\theta = \frac{\pi}{12}$

$\psi = \frac{\pi}{6}$

FIGURE 15b

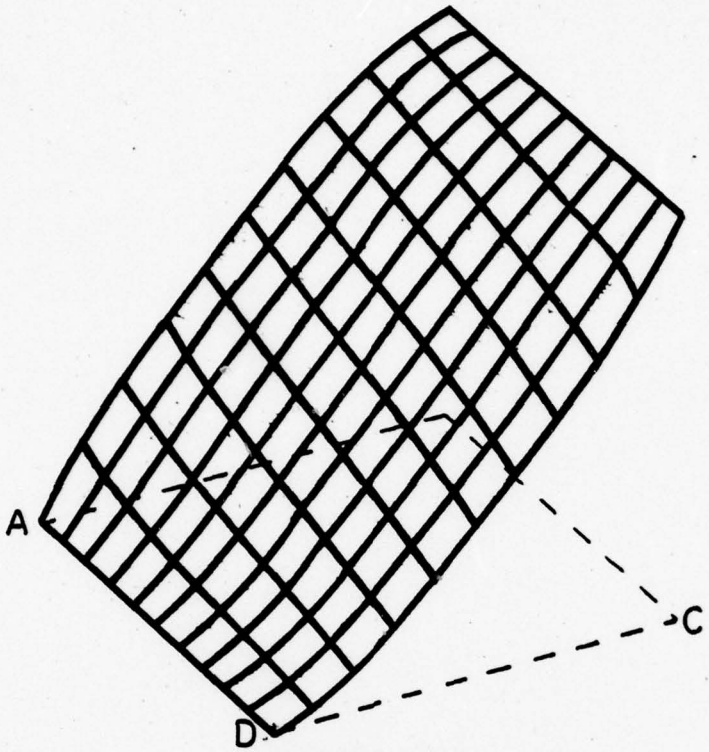

$\theta = \frac{\pi}{12}$

$\psi = \frac{\pi}{3}$

FIGURE 15c

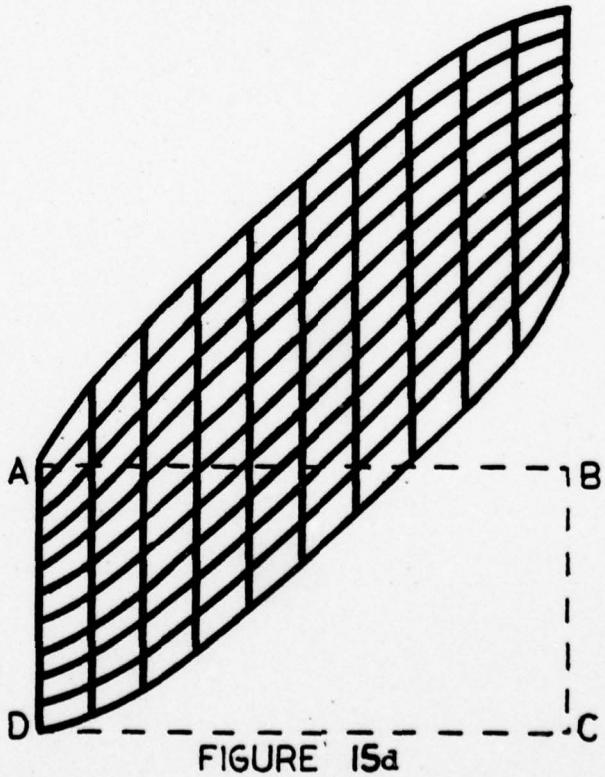

$\theta = \frac{\pi}{12}$

$\psi = \frac{\pi}{2}$

FIGURE 15d

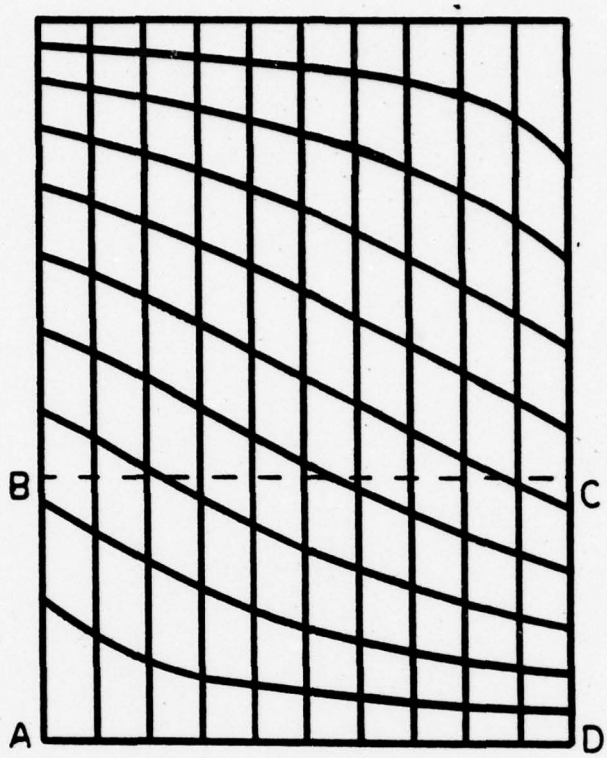

$\theta = \frac{\pi}{6}$

$\psi = 0$

FIGURE 16a

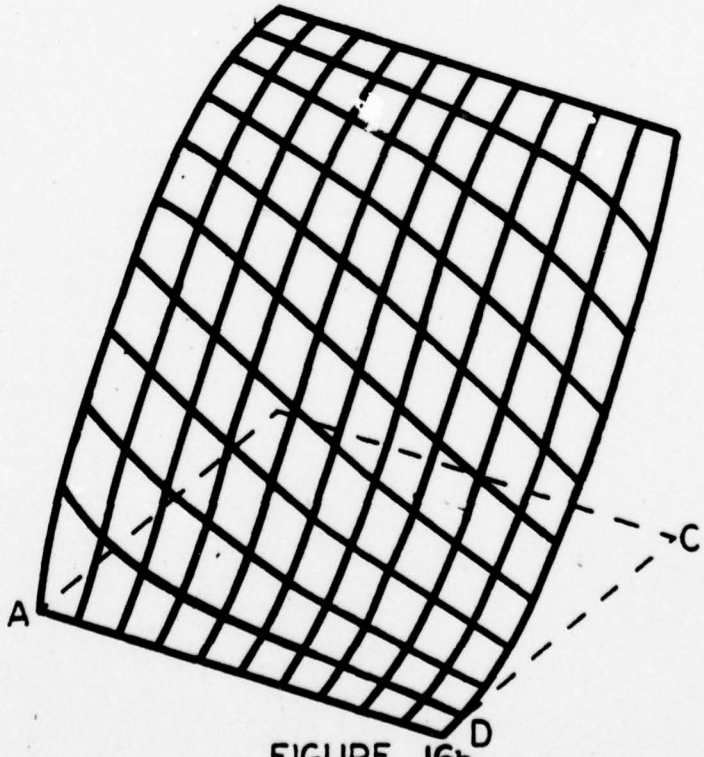

$\theta = \frac{\pi}{6}$

$\psi = \frac{\pi}{6}$

FIGURE 16b

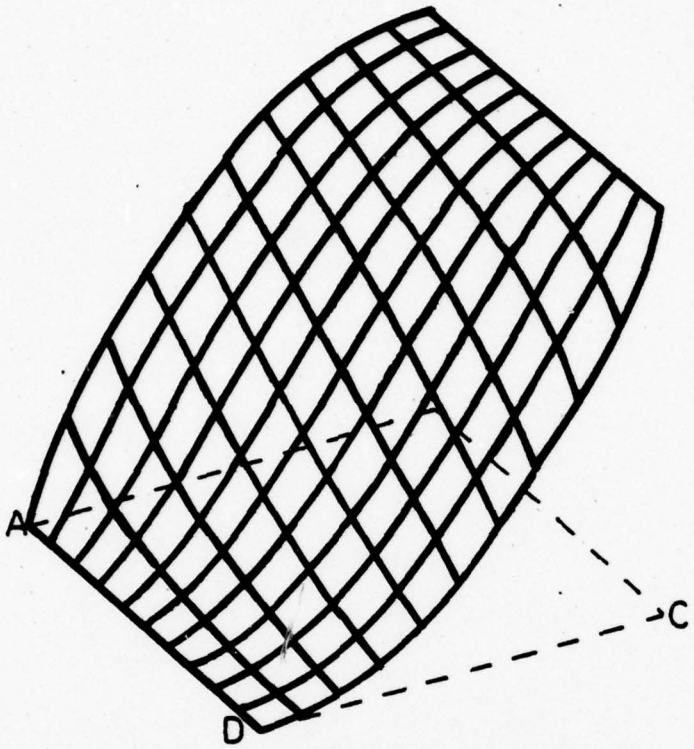

$\theta = \frac{\pi}{6}$

$\psi = \frac{\pi}{3}$

FIGURE 16c

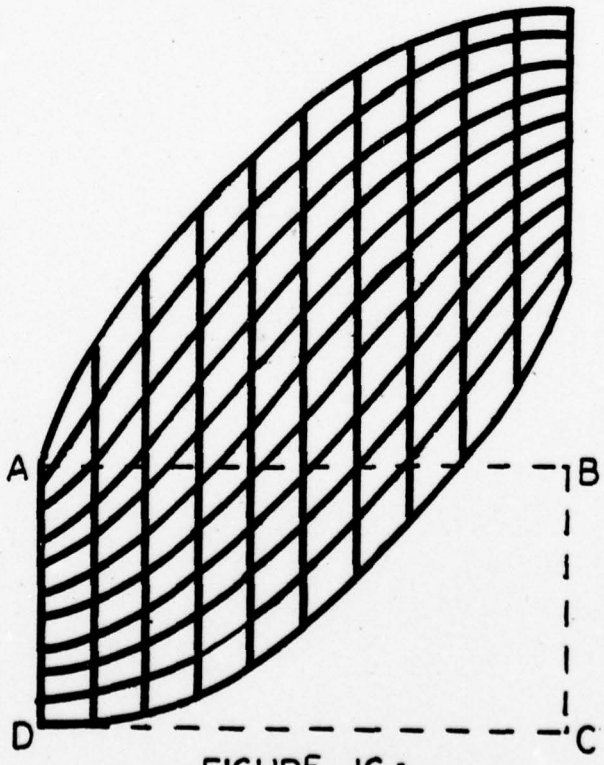

$\theta = \frac{\pi}{6}$

$\psi = \frac{\pi}{2}$

FIGURE 16d

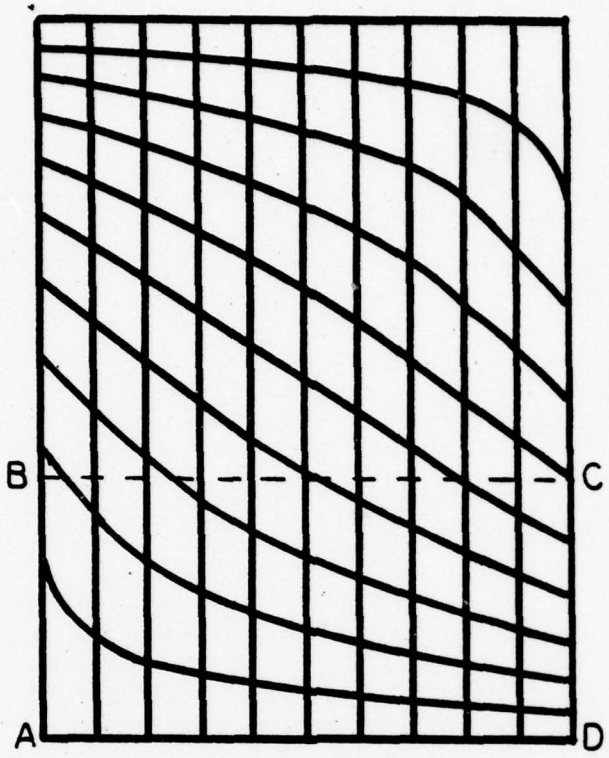

$\theta = \frac{\pi}{4}$

$\psi = 0$

FIGURE 17a

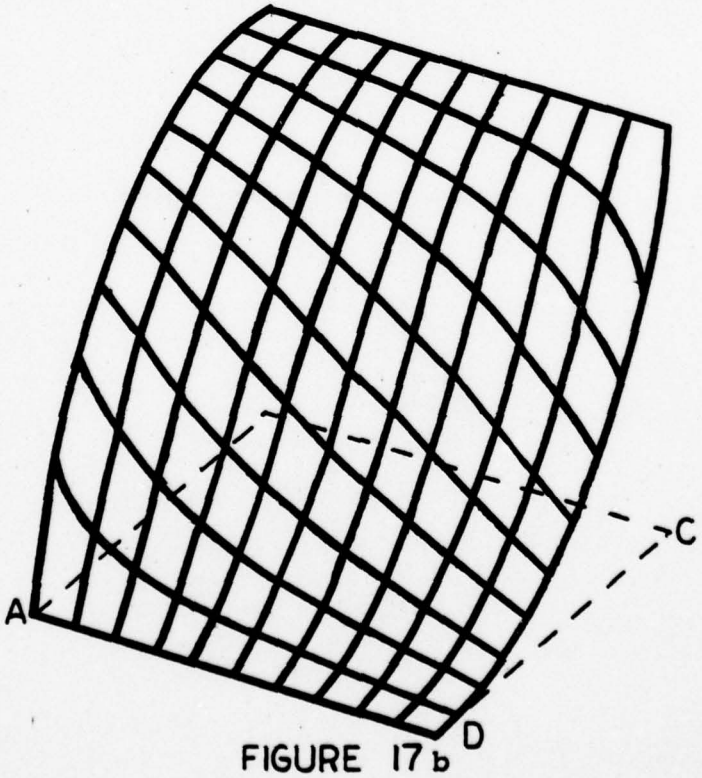

$\theta = \frac{\pi}{4}$

$\psi = \frac{\pi}{6}$

FIGURE 17b

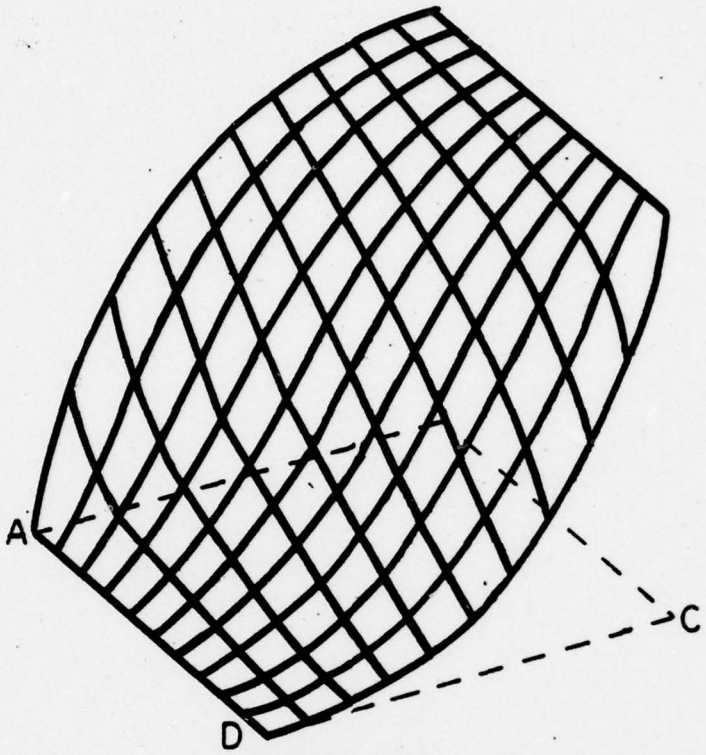

$\theta = \frac{\pi}{4}$

$\psi = \frac{\pi}{3}$

FIGURE 17c

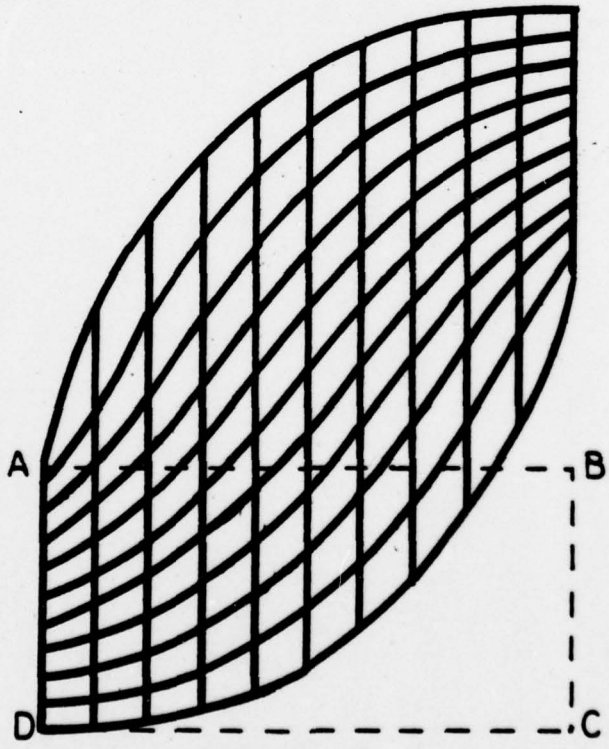

$\theta = \frac{\pi}{4}$

$\psi = \frac{\pi}{2}$

FIGURE 17d

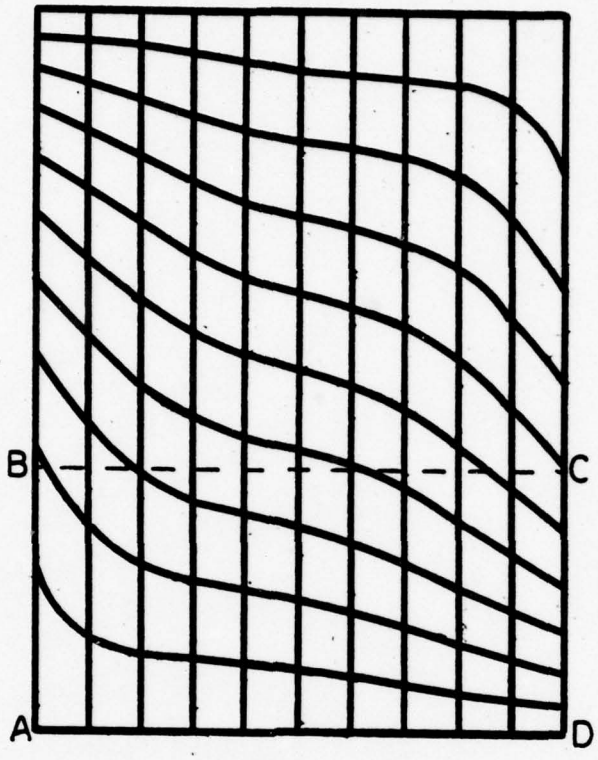

$\theta = \frac{\pi}{3}$

$\psi = 0$

FIGURE 18a

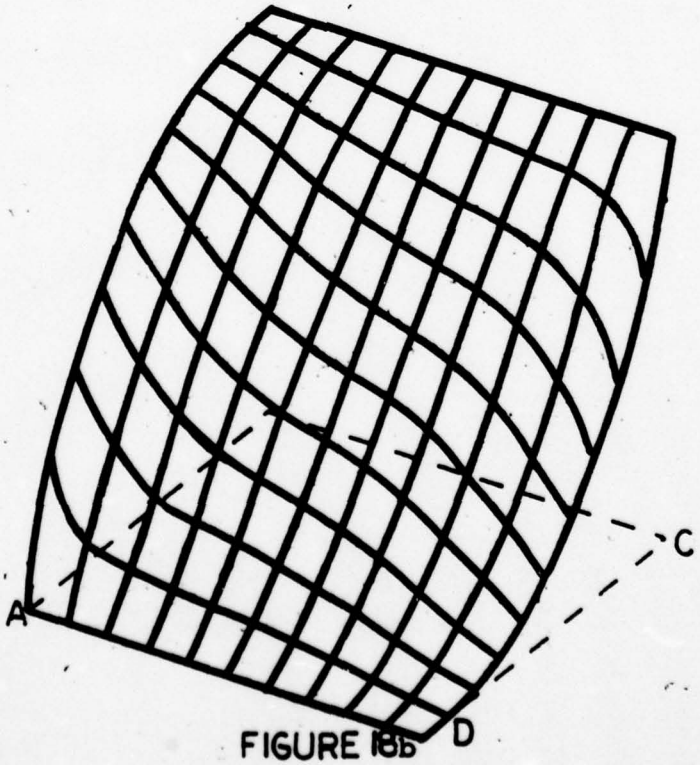

$\theta = \frac{\pi}{3}$

$\psi = \frac{\pi}{6}$

FIGURE 18b

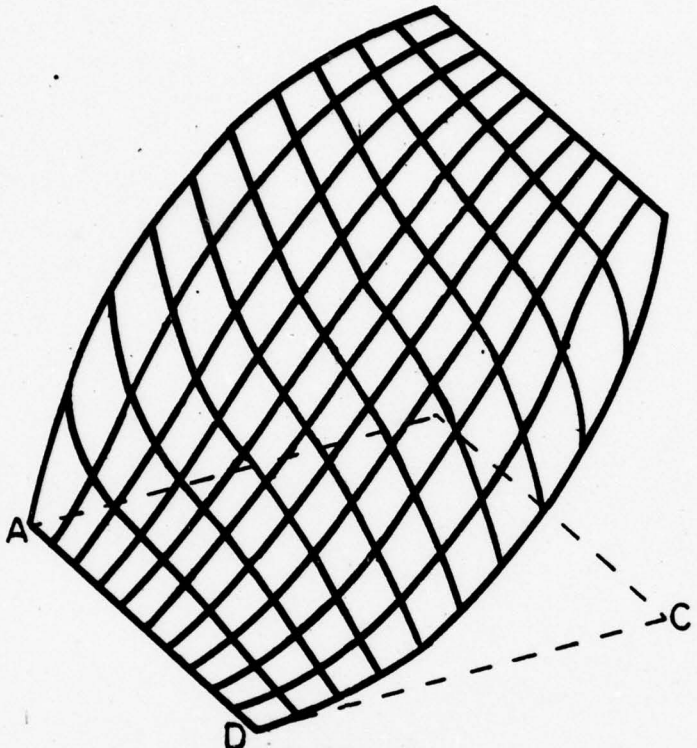

$\theta = \frac{\pi}{3}$

$\psi = \frac{\pi}{3}$

FIGURE 18 c

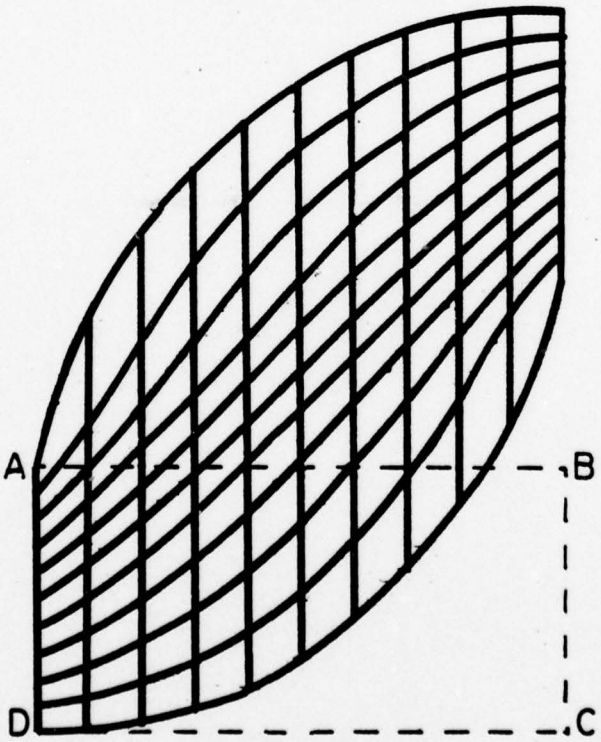

$\theta = \frac{\pi}{3}$

$\psi = \frac{\pi}{2}$

FIGURE 18 d

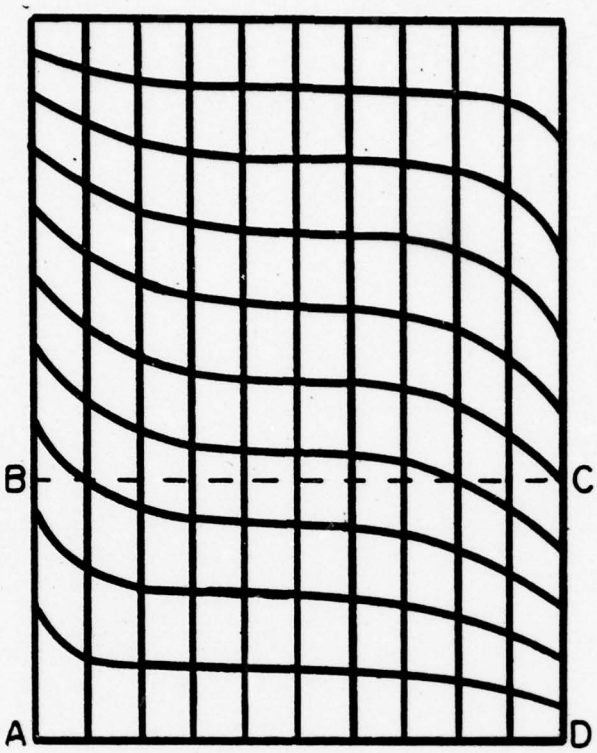

$\theta = \frac{5\pi}{12}$

$\psi = 0$

FIGURE 19a

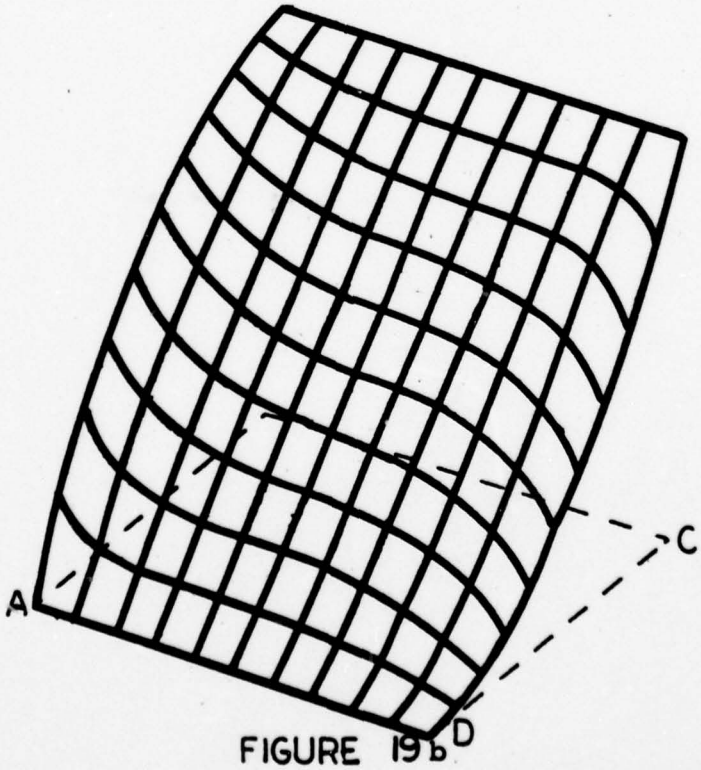

$\theta = \frac{5\pi}{12}$

$\psi = \frac{\pi}{6}$

FIGURE 19b

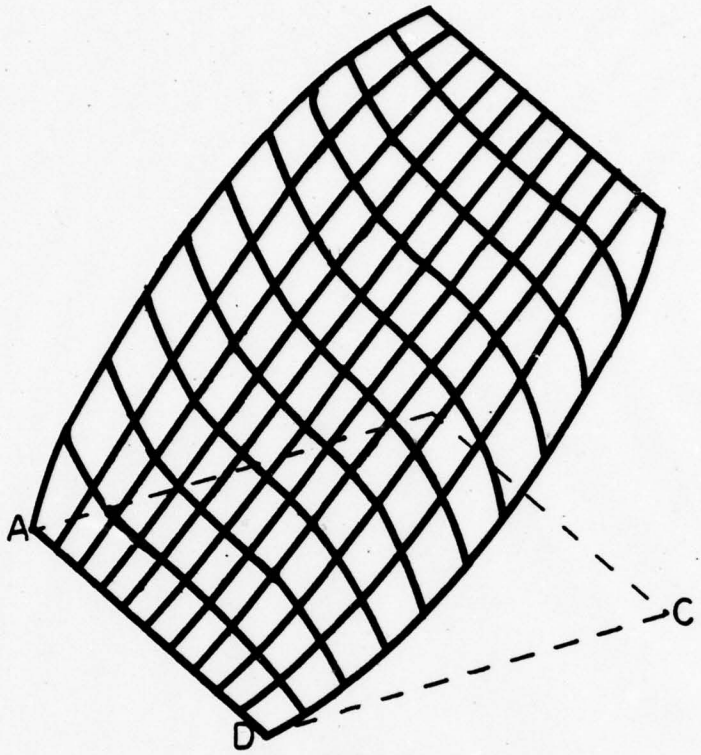

$\theta = \frac{5\pi}{12}$

$\psi = \frac{\pi}{3}$

FIGURE 19c

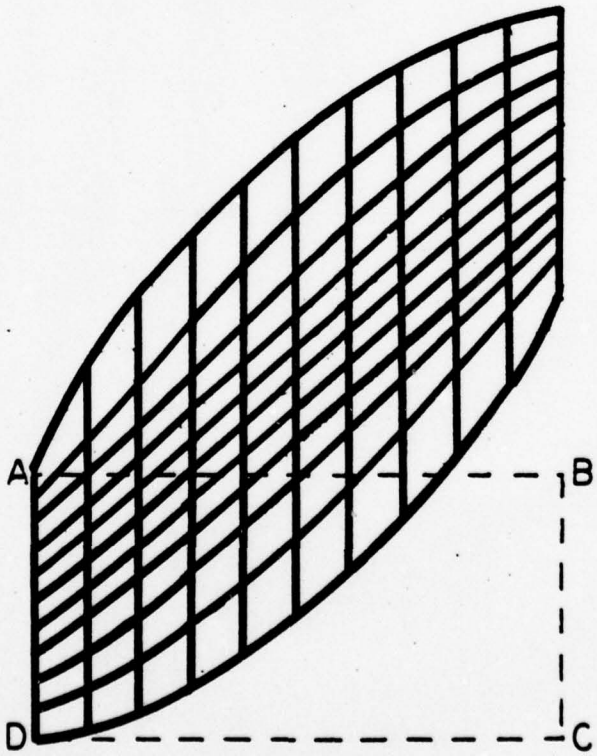

$\theta = \frac{5\pi}{12}$

$\psi = \frac{\pi}{2}$

FIGURE 19d

All connections between gridwork nodes were made by spline function fits along lines of constant x_i and all solutions were obtained from a QSFBIE with a 4-point Legendre Gauss rule for numerical quadrature.

3.2 PLANE ANISOTROPIC ELASTICITY

3.2.1 Application of Boundary Integral Equation Formulation

For the problem of plane anisotropic elasticity the governing differential equation is of the form

$$a_{ijk\ell} \frac{\partial^2 \phi k}{\partial x_j \partial x_\ell} = 0 \qquad \begin{matrix} j,\ell = 1,2 \\ i,k = 1,2,\ldots N \end{matrix}$$

where N can be 2 or 3. The significance of the two possible values for N lies in the fact that the principal axes of the material need not be parallel to the x_1-x_2 plane. In other words, the three rotational angles necessary to describe the material constants in terms of the problem coordinates x_j can all be varied. Consequently, for N=3, the antiplane problem is also solved in addition to the plane problem (N=2). We note here that if a plane problem is posed as a problem with N=3 there will be repeated roots of (2.8) making the characteristic vectors $A_{k\alpha}$ of (2.7) non-unique. However, the plane and antiplane problems in this case are uncoupled and two of the characteristic vectors can be chosen arbitrarily. Furthermore, note that for the case of an isotropic material the characteristic roots p_α(α=1,2,...N) occur

as repeated roots from (2.8). Consequently the $A_{k\alpha}$ are not unique, nor is there any uncoupling, leading to a breakdown of the procedure.

As in the case of plane anisotropic heat conduction, the sequence of solution of the characteristic variables (p_α, $A_{k\alpha}$, $N_{\alpha j}$, $L_{ij\alpha}$, d_j, and D_α) is the same; but the complexity of the calculations do not allow us to write out explicit expressions for them. The formation of the Φ_{ij} kernel is then straightforward per (2.18), but the assembly of the Γ_{ij} by (2.4) involves four nested loops which may be reduced to two by the following procedure utilizing $L_{ij\alpha}$. We have identified the real solution ϕ_k by (2.9) as

$$\phi_k = \sum_\alpha A_{k\alpha} f_\alpha(z_\alpha) + \sum_\alpha \bar{A}_{k\alpha} \bar{f}_\alpha(\bar{z}_\alpha) \qquad (3.18)$$

Now P_i can be written from (2.4) as

$$P_i = \left(a_{ijk1} \frac{\partial \phi_k}{\partial x_1} + a_{ijk2} \frac{\partial \phi_k}{\partial x_2}\right) n_j \qquad (3.19)$$

Taking the derivatives indicated by (3.19) on ϕ_k as given by (3.18) yields

$$P_i = \sum_\alpha [(a_{ijk1} + a_{ijk2} p_\alpha) A_{k\alpha}] f'_\alpha(z_\alpha) n_j + \sum_\alpha [(a_{ijk1} + a_{ijk2} \bar{p}_\alpha) \bar{A}_{k\alpha}] \bar{f}'_\alpha(\bar{z}_\alpha) n_j \qquad (3.20)$$

We recognize the quantities in brackets as $L_{ij\alpha}$ so that we may write (3.20) as

$$P_i = [\sum_{\alpha} L_{ij\alpha} f'_{\alpha}(z_{\alpha}) n_j + \sum_{\alpha} \bar{L}_{ij\alpha} \bar{f}'_{\alpha}(\bar{z}_{\alpha})] n_j \quad (3.21)$$

Finally

$$f'_{\alpha}(z_{\alpha}) = \frac{1}{2\pi i} \frac{D_{\alpha}}{(z_{\alpha} - c_{\alpha})}$$

$$\bar{f}'_{\alpha}(\bar{z}_{\alpha}) = \frac{1}{2\pi i} \frac{\bar{D}_{\alpha}}{(\bar{z}_{\alpha} - \bar{c}_{\alpha})}$$

so that P_i can be expressed as

$$P_i = \frac{1}{2\pi i} \left\{ \sum_{\alpha} L_{ij\alpha} \frac{D_{\alpha}}{(z_{\alpha}-c_{\alpha})} - \sum_{\alpha} L_{ij\alpha} \frac{\bar{D}_{\alpha}}{(\bar{z}_{\alpha}-\bar{c}_{\alpha})} \right\} n_j \quad (3.22)$$

Thus when we assemble Γ_{ij}, it assumes the form

$$\Gamma_{ij} = \frac{1}{2\pi i} \left\{ \sum_{\alpha} L_{ik\alpha} \frac{D_{\alpha j}}{(z_{\alpha}-c_{\alpha})} - \sum_{\alpha} L_{ik\alpha} \frac{\bar{D}_{\alpha j}}{(\bar{z}_{\alpha}-\bar{c}_{\alpha})} \right\} n_k \quad (3.23)$$

3.2.2 Solved Problems

In this section we wish to demonstrate the ability of the method to solve problems of physical significance reliably and indicate the stability of the method as the governing differential equation we are trying to solve

becomes parabolic. As in the problems solved in section 3.1.2, essential parameters of the particular problems are varied to demonstrate the ability of the method to discern the variation. The solved problems considered in this section deal only with the case of N=2.

(a) Consider a general anisotropic rectangular plate of dimensions 2ℓ x $2w$ in simple tension as shown in Figure 20. The exact solution for ℓ=w=a with

$$u_1(-a,-a) = u_2(-a,-a) = u_{1,2}(-a,x_2) = 0$$

is

$$u_1 = s_{11}(x_1 + a)$$

$$u_2 = (s_{12}(x_2 + a) + s_{16}(x_1 + a))$$

where s_{ij} represent material compliances in contracted notation. Note that for the case of general anisotropy

$$u_2 = u_2(x_1, x_2)$$

because of the s_{16} term. A non-zero s_{16} term may be obtained by rotating any material other than isotropic (or transversely isotropic about the x_1-x_2 plane) through an arbitrary angle θ about the x_3 axis. In certain material classes $\theta=m\pi/2$ (m=0,1,2,...) will not provide

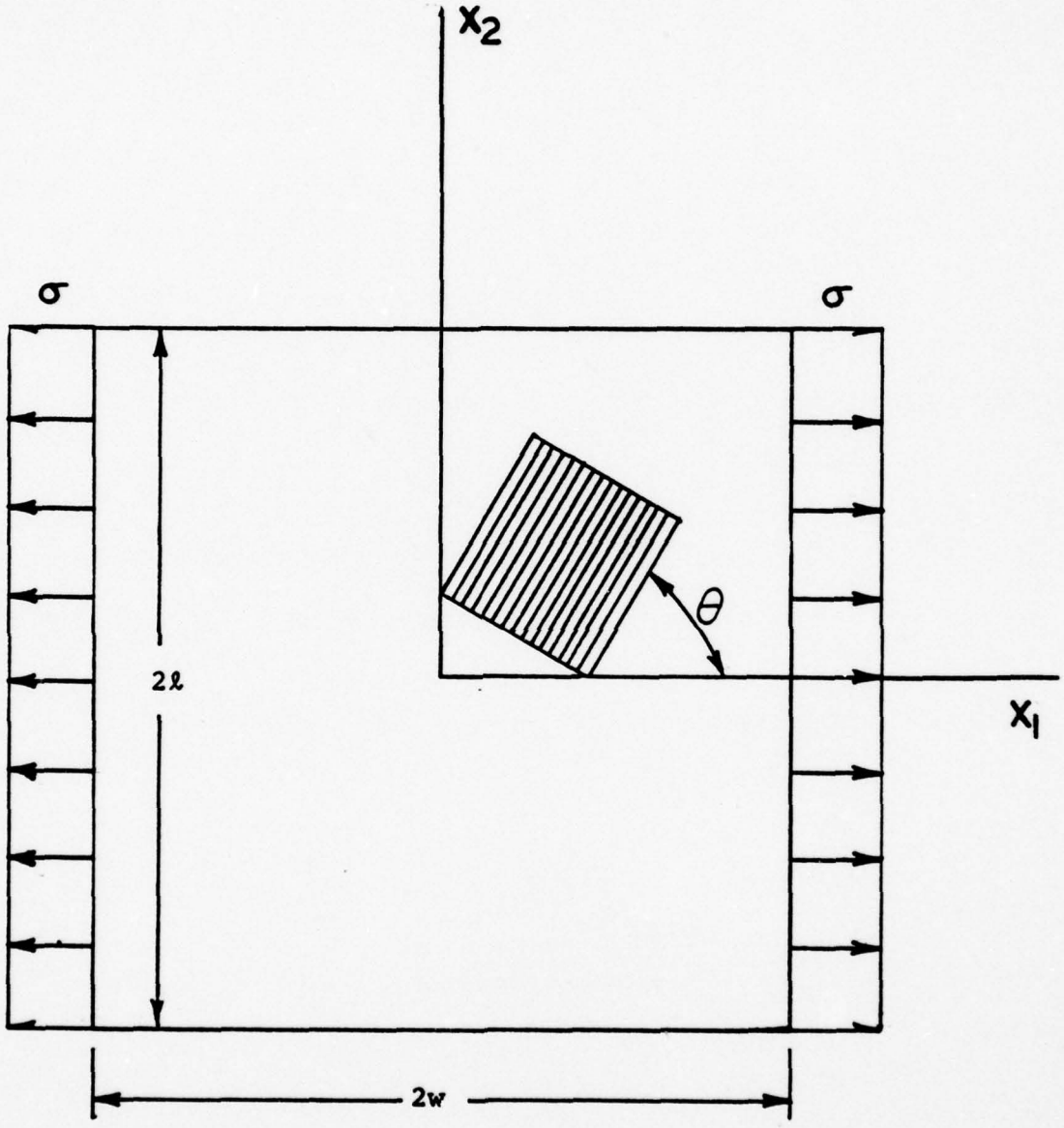

FIGURE 20

a non-zero s_{16} term, but such cases will not be considered here. Accordingly, the simplest choice is that of a transversely isotropic material which does not have symmetry about $x_3=0$. This material will have 5 independent material constants, only four of which will enter into the x_1-x_2 plane problem, namely c_{1111}, c_{2222}, c_{1122}, and c_{1212}. For convenience we shall denote them in the following manner

$$A = c_{2222}$$

$$C = c_{1111}$$

$$F = c_{1122}$$

$$L = c_{1212}$$

The determinant polynomial (2.8) for this type of material aligned in the x_1-x_2 coordinate axes (i.e., $\theta=0$) may be written in explicit terms as

$$ALp^4 - (F^2 + 2FL - AC)p^2 + CL = 0 \qquad (3.24)$$

The biquadratic roots of (3.24) are

$$p^2 = \frac{(F^2+2FL-AC) + i\sqrt{4ACL^2-(F^2+2FL-AC)^2}}{2AL} \qquad (3.25)$$

Examination of the approach of the discriminant of (3.25) to zero shows the approach of the elliptic system of this

particular problem to becoming parabolic. We may observe the approach analytically by putting

$$A = \eta$$

$$C = 3\eta/2$$

$$F = \eta/10$$

$$L = \eta/5$$

and let η=9,8,7,...1 to cause the discriminant to approach zero while satisfying the ellipticity requirement (equation (2.3)). In such a manner, the accuracy of the solution procedure as well as the stability of it can be demonstrated.

The results of this survey with $a=\sigma=1$ are summarized in Table 3. The average absolute error (ϵ_Ψ) has a similar interpretation as in section 3.1.2 except that Ψ of equation (3.8) represents either tractions ($\underset{\sim}{t}$) or displacements ($\underset{\sim}{u}$) here. All solutions were obtained using one segment per side in a QSFBIE (8 nodes total) with 4-point Legendre Gauss rule for numerical quadrature.

(b) Consider an elastic anisotropic plate bounded by two hyperbolas and two equal rectilinear sections subject to uniform tensile loading (σ) in the direction of the normal on the rectilinear sections (Figure 21). For a plate of infinite extent in the x_1 directions, with axes as shown, the hyperbolic edges will be given by

TABLE 3

AVERAGE ABSOLUTE ERRORS x 10^4

$\theta = \pi/4$

η	DISCRIMINANT	TRACTIONS	DISPLACEMENTS
9	-12220.	122	116
8	-7628.8	122	116
7	-4471.9	122	116
6	-2413.8	122	116
5	-1164.1	122	116
4	-476.8	122	116
3	-150.86	122	116
2	-29.80	122	116
1	-1.8625	122	116

$$\frac{x_2^2}{a^2} - \frac{x_1^2}{b^2} = 1$$

The variable of interest in this problem is the distribution of σ_{11} at the narrowest section (i.e., along $x_1=0$). The geometry of the plate is characterized by defining $c=a/b$, which is the governing parameter of the stress distribution in the plate for a given material. An approximate solution for the stress distribution of the general anisotropic plate is given by Lekhnitskii [6] from which we compare normal stress distributions along the narrowest cross section. If we choose an orthotropic material with its principal directions (i.e., fiber direction angle θ of Figure 21 equal to $m\pi/2$, $m=0,1,2,...$) we may use quarter-symmetry to pose the problem as depicted in Figure 22 and obtain the normal stress distribution directly from the boundary solution tractions. The parameter x_1^* (Figure 22) represents the finite length of the plate used for the numerical solution modelling.

The BIE solution is compared with the approximate solution for an orthotropic material having stiffnesses (in units of $lb/[in^2 \cdot 10^6]$) $c_{11}=1.2035$, $c_{22}=0.60176$, $c_{12}=0.04276$, and $c_{66}=0.0699$, which are constants (cf.[6]) for a type of plywood. The problem was posed with $\sigma=a=x_1^*=1$, $c=1/10$, $1/2$, 1, 2 for $\theta=0$ and $\theta=\pi/2$. Comparison stress distributions are shown in Figures 23-26, in which the applied traction is shown on the right hand side

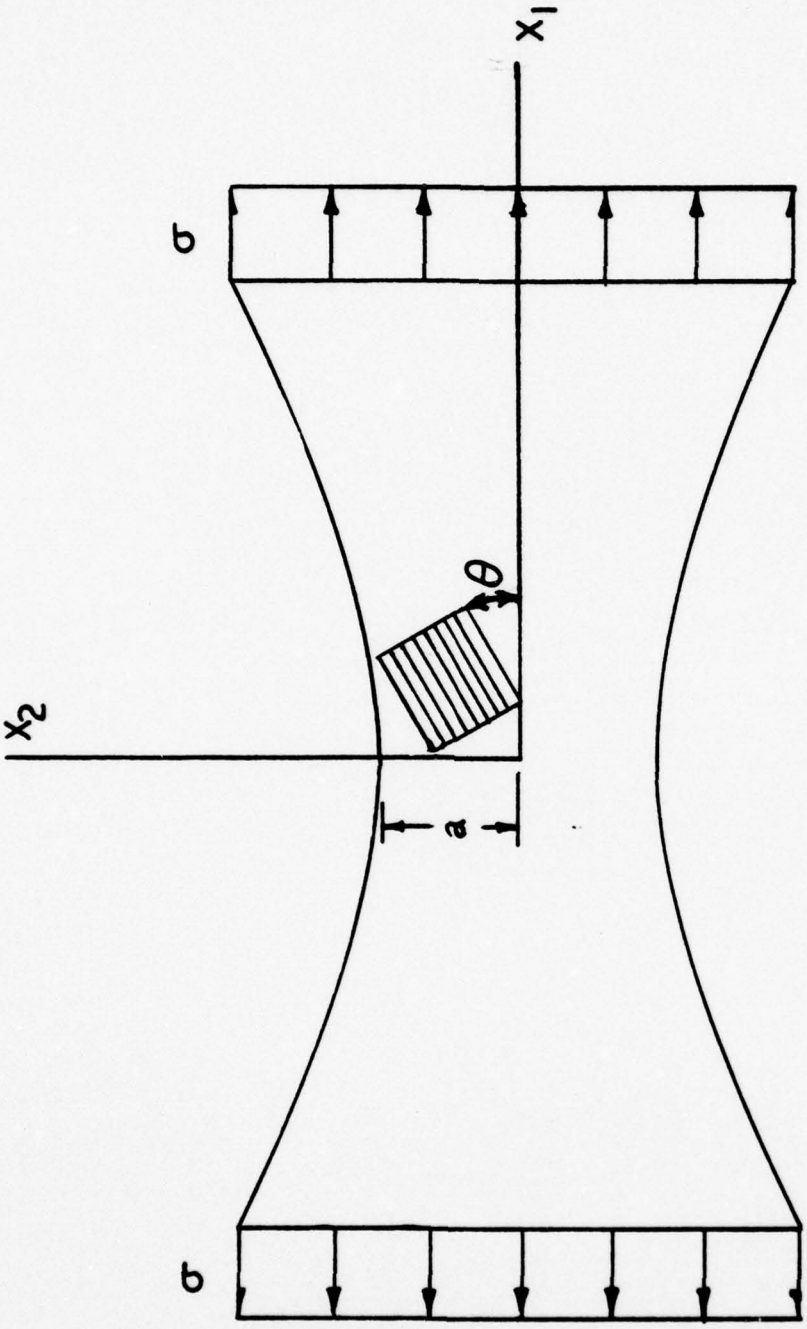

FIGURE 21

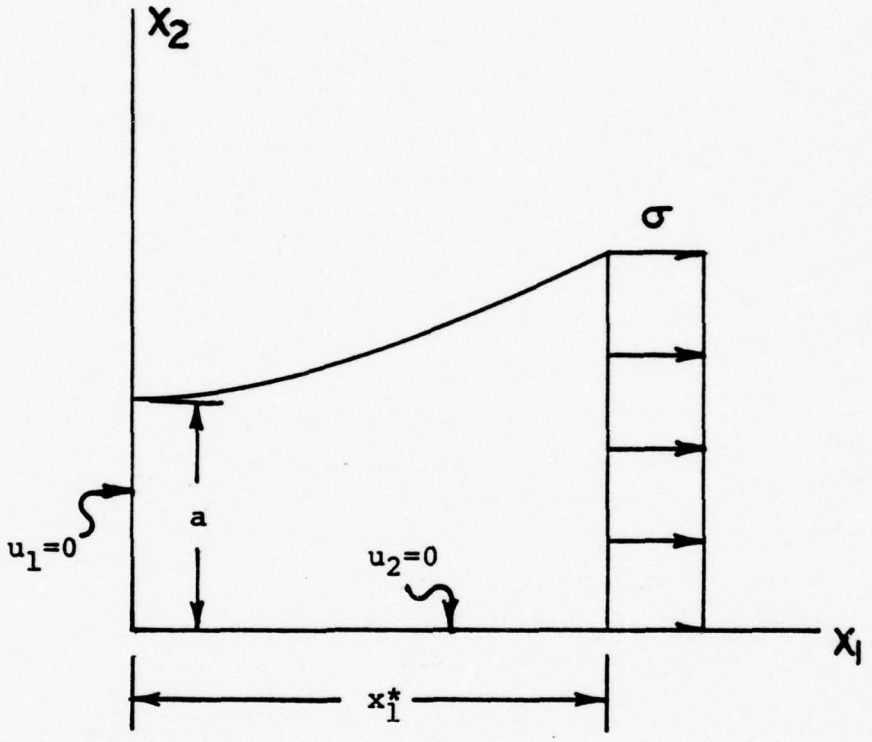

FIGURE 22

to serve as an indication of the magnitude of the stress concentration. The reliability of the method is emphasized by the crude discretizations of the problem of one and two segments per side in a QSFBIE (8 and 16 nodes respectively). All solutions were obtained using a 4-point Legendre Gauss rule for numerical quadrature.

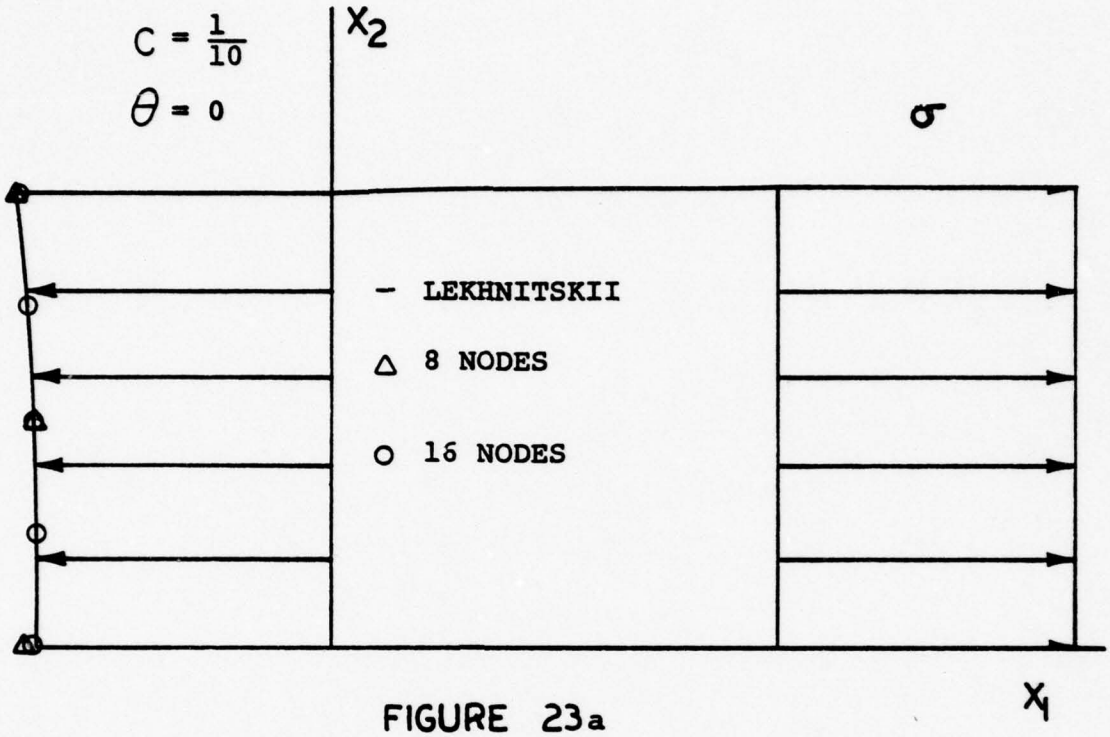

FIGURE 23a

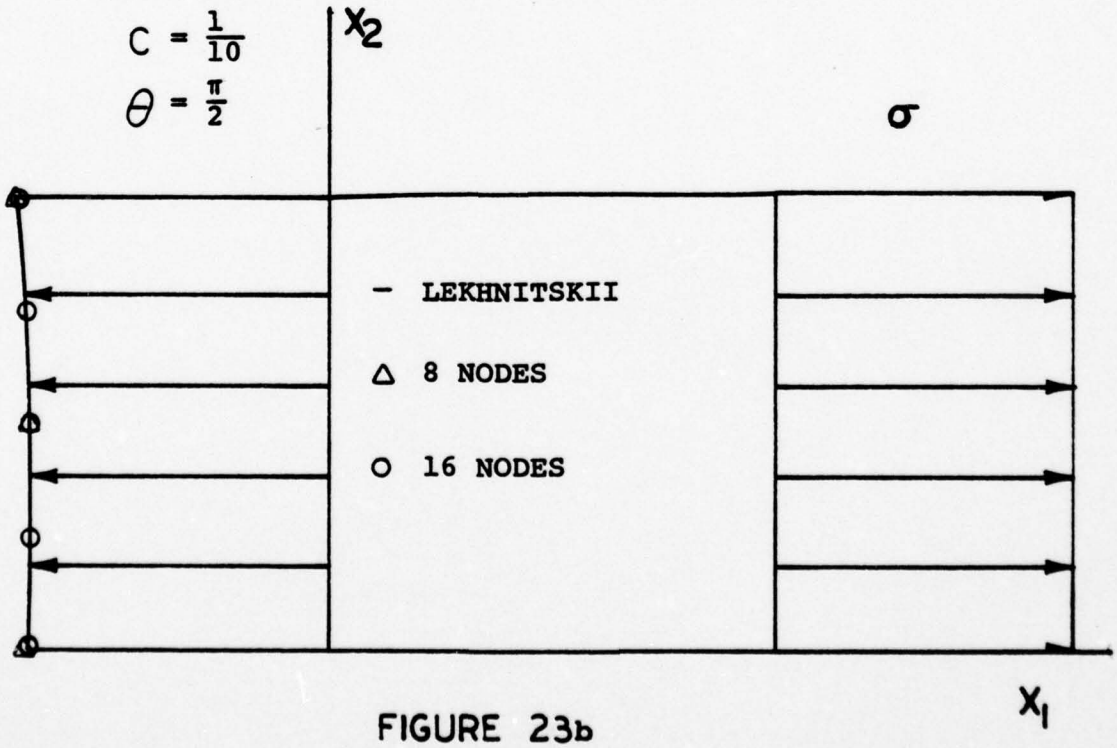

FIGURE 23b

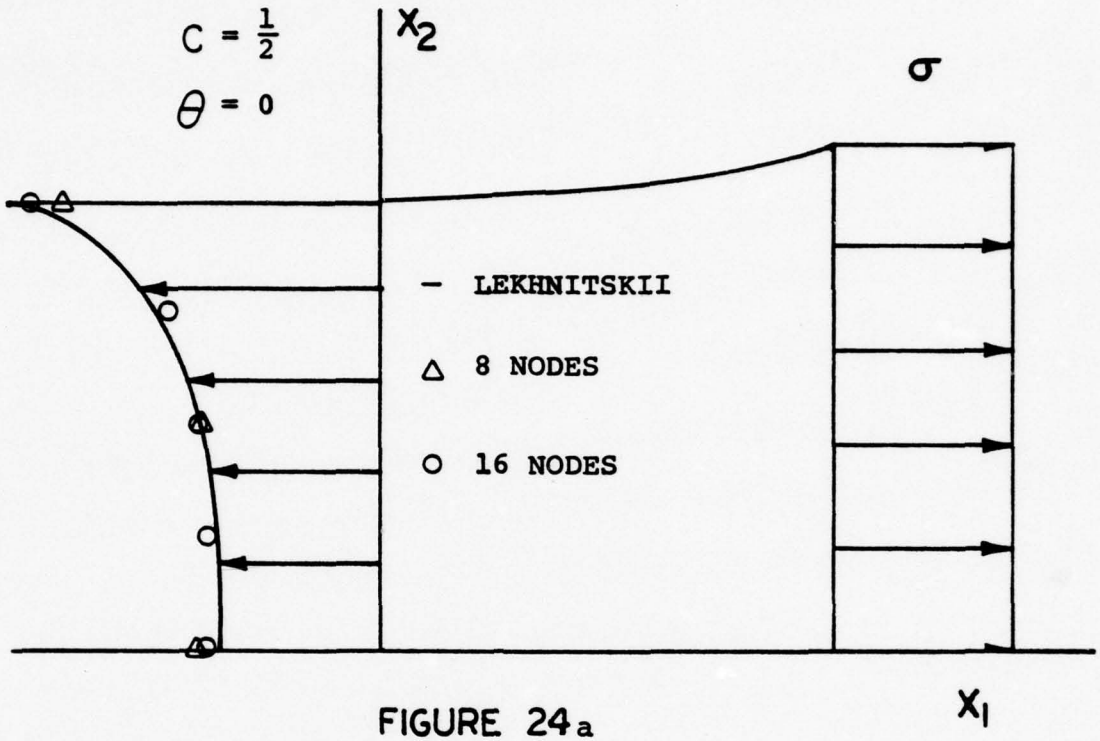

FIGURE 24a

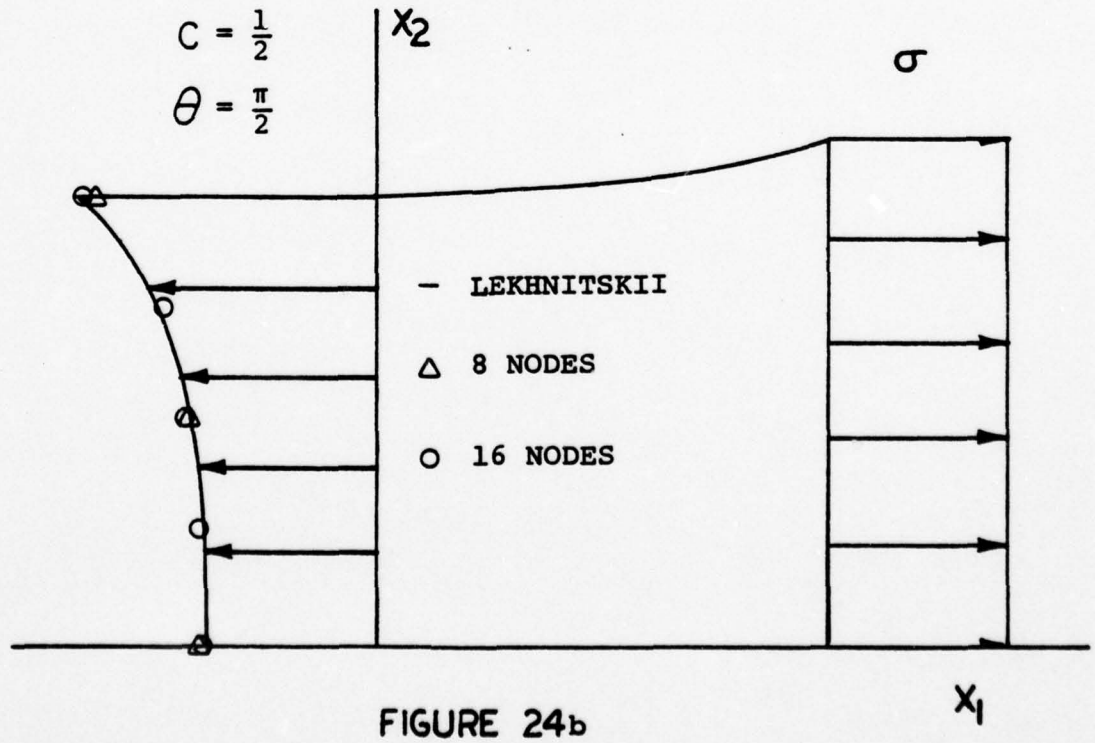

FIGURE 24b

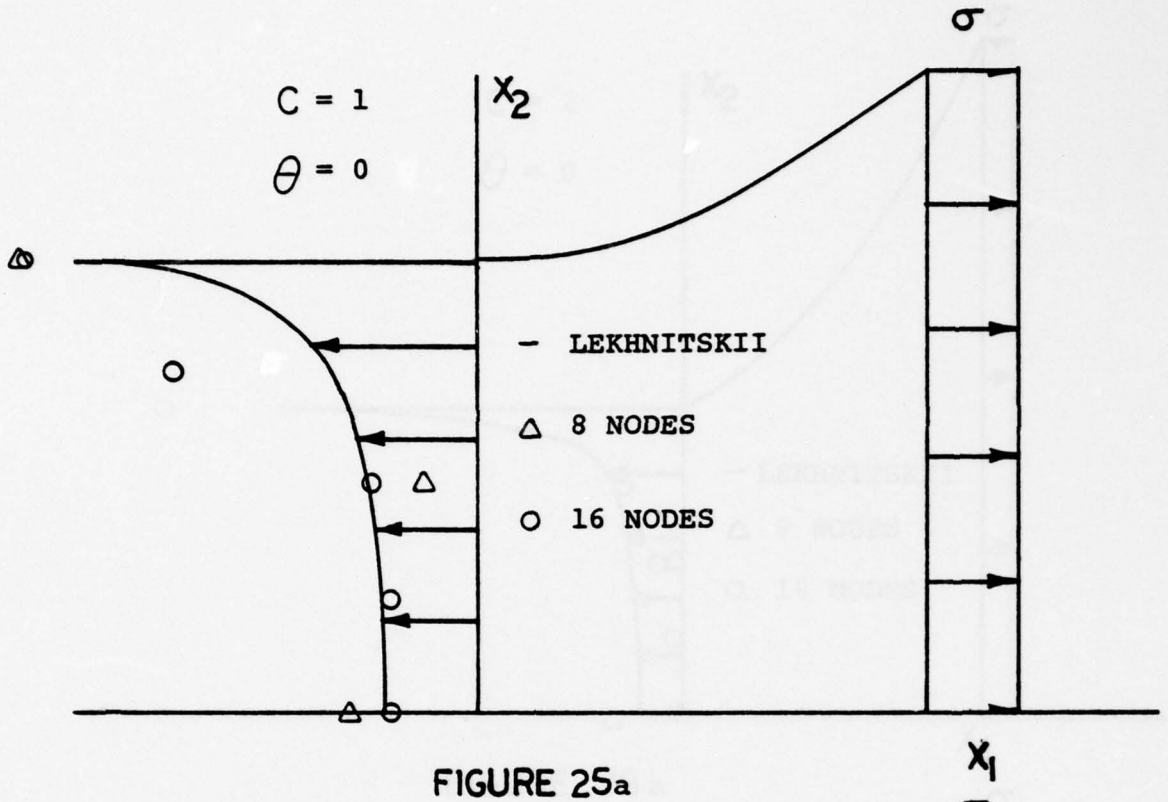

FIGURE 25a

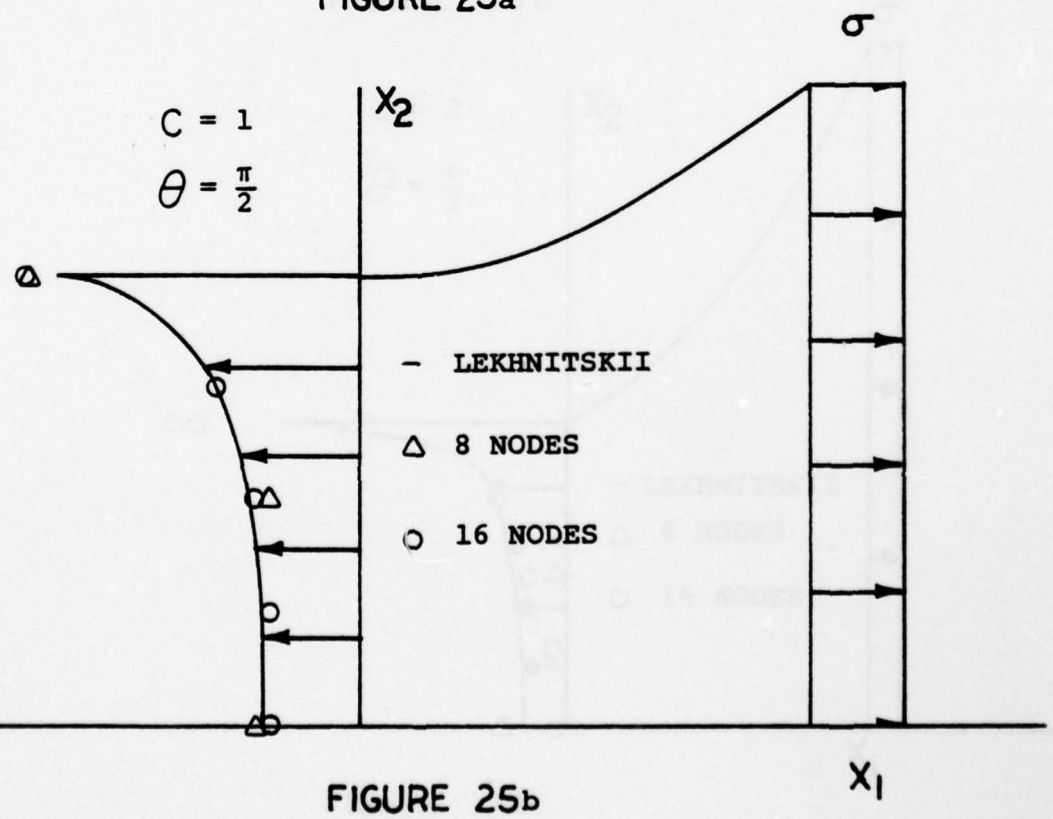

FIGURE 25b

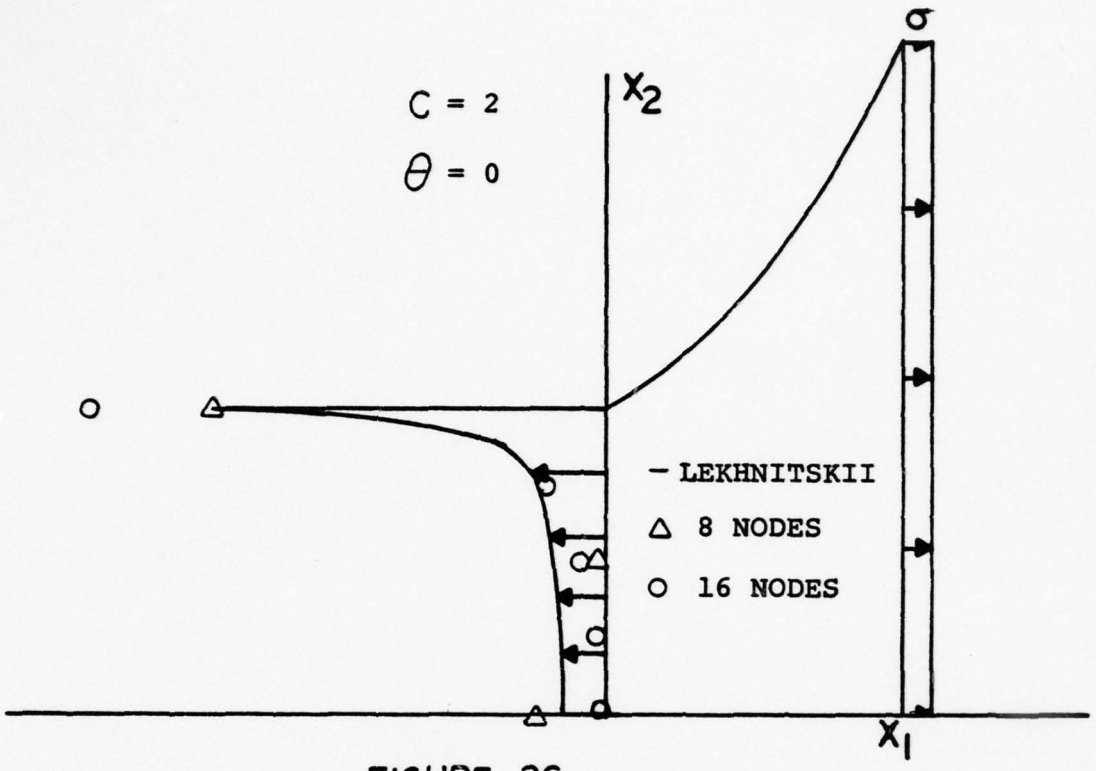

FIGURE 26a

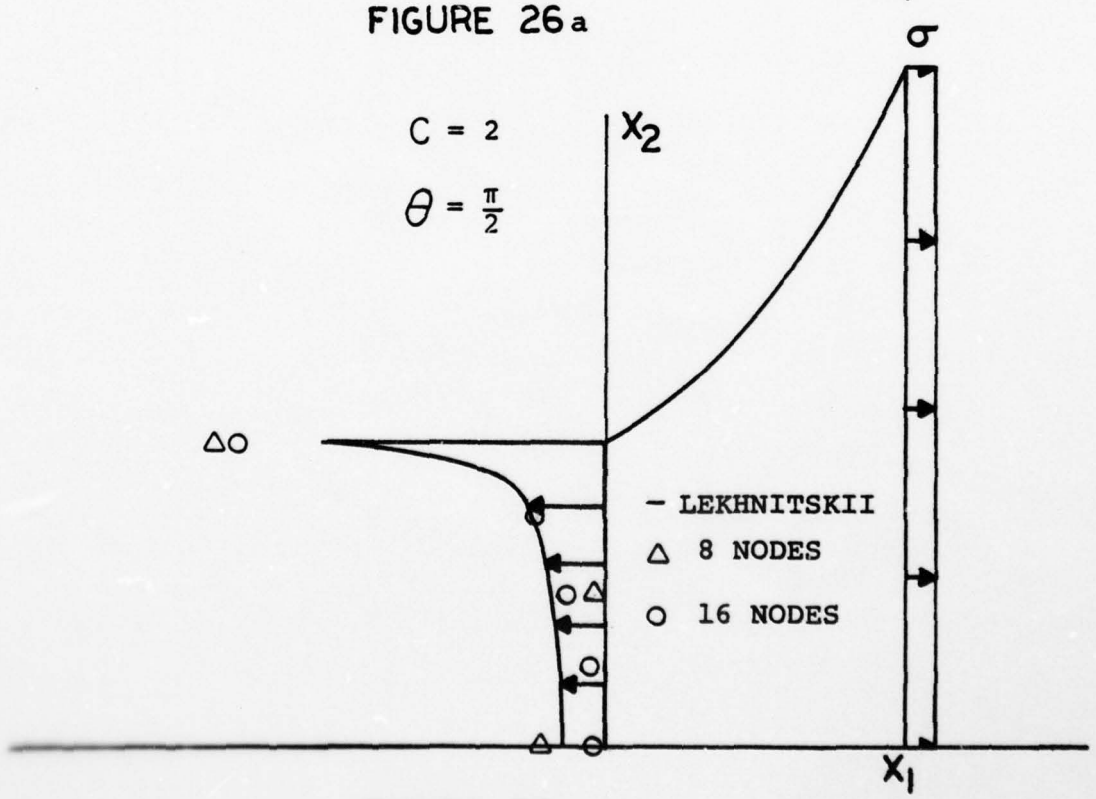

FIGURE 26b

CHAPTER FOUR

DISCUSSION AND CONCLUSIONS

The purpose of the work in this thesis is: (1) to develop the algorithm derived by Clements and Rizzo for the solution of boundary value problems governed by a system of second order linear elliptic partial differential equations into an explicit numerical procedure; (2) verify the numerical procedure by comparing numerical solutions by it with exact solutions.

The first purpose is motivated by the need to solve the title problems numerically coupled with the fact that the boundary integral equation method is especially well suited for problems governed by linear elliptic partial differential equations [7], [8]. The advantage of the BIE method over other numerical methods such as the Finite Difference Method (FDM) and the Finite Element Method (FEM) in attacking the title problems is that the numerical process of the BIE method is involved only with the one-dimensional bounding curve or curves. This serves to greatly reduce the amount of data preparation and computer core and time requirements, especially when the ratio of the circumference to the area of the domain is relatively low. The amount of reduction is dependent on the degree of the polynomial shape function (γ) necessary to approximate boundary geometry and boundary variables appropriately. In practice, quadratic shape function

approximations represent boundary geometry and boundary variables well, while providing adequate convergence for decreasing mesh length interval [9], [10]. The error analysis for the piecewise quadratic Lagrange's polynomial approximation [11] shows

$$||f - p|| \leq \frac{||f^{III}||h^3}{12}$$

where f is the function to be approximated, p_2 is the piecewise quadratic Lagrange's interpolating polynomial, and h is the mesh length interval between nodes.

One should note that although computer core requirements will be less for the BIE method than for a numerical method such as the FEM, the coefficient matrix involved (cf. section 2.3.4) is a full matrix unlike the banded sparse matrix of the FEM. This is an undesirable computational feature.

As to the second purpose, the test problems of Chapter 3 demonstrated the ability of the numerical procedure to solve problems of significance reliably. Moreover, the accuracy of the solution procedure as the partial differential equations became weakly elliptic was demonstrated through analytic surveys. All the problems presented were run on an IBM 370 Model 165 computer.

It is appropriate at this time to make some remarks regarding the algorithm derived by Clements and Rizzo. The most significant aspect of the algorithm is its

generality of application to second order linear elliptic systems. Furthermore, the conciseness of the formulation makes the numerical interpretation of the algorithm a straightforward procedure. However, the algorithm does not represent the first application of the BIE method to problems involving anisotropy.

The application of the BIE to plane anisotropic elastic bodies was first performed by Rizzo and Shippy [12]. Their formulation was based on the stress field due to a point force in an infinite sheet of anisotropic elastic material obtained by A.E. Green [13]. Green's point force solution is derived from a stress function form which places certain constraints on material constants in order that the material be admitted within the stress function. Nonetheless, a large number of materials satisfy the constraints, and Rizzo and Shippy obtained excellent agreement between the numerical values obtained from a piecewise constant BIE (employing numerical quadrature of the necessary integrals) and those obtained from analytical solutions in direct comparisons.

The BIE method has also been applied to two dimensional plane stress problems for fully anisotropic elastic materials by Cruse [14]. His development of the boundary integral equations follows from the notation and theoretical development of the field equations as given by Lekhnitskii [15]. Cruse attained excellent agreement between available exact analytical solutions and numerical

solutions from a piecewise linear BIE (utilizing exact integration of the resulting necessary integrals). Note that the development of the BIE based on the theoretical development of Lekhnitskii requires that the principal axes of the material be located in the x_1-x_2 plane of the problem, whereas the algorithm of Clements and Rizzo allows the material to assume a completely arbitrary orientation. This arbitrary orientation of the material induces coupling of the plane and antiplane problems, so that the problem must be solved with N=3. Consequently, the size of the coefficient matrix (cf. section 2.3.4) necessarily expands from [2n x 2n] to [3n x 3n], where n is the total number of nodes in the problem's modelling for the numerical solution by the BIE.

The plane stress problems of practical interest usually involve the principal axes being located in the x_1-x_2 plane, making the arbitrary material orientation feature of the algorithm an available convenience when necessary. A more practical application of the case of N=3 is the bending of plates weakened by openings under antiplane loading distributed along the edge. Lekhnitskii [6] gives extensive treatment of this type of problem, which was not considered in the solved problems of this thesis.

One type of plane stress problem of practical interest is that of plates weakened by openings subject to various in-plane loading conditions. For this type

of problem the variable of interest is the hoop stress distribution around the opening. Inherently the boundary solution stress variables in the BIE method are the tractions from which the hoop stresses cannot be determined. Moreover, we cannot obtain an expression for $\partial u_i/\partial x_j$ ($i=1,2,...N$; $j=1,2$) directly because the numerical processes of the PSFBIE deal with the mapped coordinate ξ. However, we may establish a system of simultaneous linear algebraic equations to solve for the stress system at the point in question. The stress system may then be rotated through the necessary angles via Mohr's circle to obtain the oblique stresses of interest. Appendix III outlines the procedure in the general case for N=2 or 3.

Finally, it should be observed that the work in this thesis has been performed with the idea that there is no absolute advantage of any numerical solution procedure. Therefore, the need to improve the approximations within the numerical solution procedures is frequently necessary to obtain the desired solution. The foundations of these improved approximations for the BIE method are laid within this thesis from which they may be implemented readily. Also, it is possible to generalize the methods presented in this thesis to boundary value problems governed by other differential equations, e.g., differential equations which would admit a non-zero right hand side to equation (2.1) for the case of N=1 and equations which govern inhomogenous media (inclusion problems) where conditions of continuity at the interface must be considered.

APPENDIX I

LIMIT PROCESSES FOR ESTABLISHING INTERIOR IDENTITY AND BOUNDARY INTEGRAL EQUATION

I.1 INTERIOR IDENTITY

We wish to establish an interior identity from (2.28) by deleting the neighborhood of the singular point $\underset{\sim}{x}_o$ and taking appropriate limits. To facilitate this process, let us assign explicit point dependence to the variables involved in (2.28).

$$\int_C [P_i(\underset{\sim}{X})\Phi_{ij}(\underset{\sim}{X},\underset{\sim}{x}_o) - \Gamma_{ij}(\underset{\sim}{X},\underset{\sim}{x}_o)\phi_i(\underset{\sim}{X})]dS(\underset{\sim}{X}) = 0 \qquad (I.1)$$

In classical fashion we delete a square region of sides 2ε surrounding $\underset{\sim}{x}_o$ (see Figure 1) whose contour we will denote C'. We can rewrite (I.1) as

$$\int_C [P_i(\underset{\sim}{X})\Phi_{ij}(\underset{\sim}{X},\underset{\sim}{x}_o) - \Gamma_{ij}(\underset{\sim}{X},\underset{\sim}{x}_o)\phi_i(\underset{\sim}{X})]dS(\underset{\sim}{X})$$

$$+ \int_{C'} [P_i(\underset{\sim}{X})\Phi_{ij}(\underset{\sim}{X},\underset{\sim}{x}_o) - \Gamma_{ij}(\underset{\sim}{X},\underset{\sim}{x}_o)\phi_i(\underset{\sim}{X})]dS(\underset{\sim}{X}) = 0 \qquad (I.2)$$

The first integral is identically zero by our stipulation that it does not contain $\underset{\sim}{x}_o$. Hence we need only consider

the integral over C′. For convenience we let $\underset{\sim}{x}_o$ be the origin and consider the parts of the integral separately. Substitution of equation (2.18) into (I.2) with appropriate association as outlined in section 2.2.1 leads the first part to take the form

$$\frac{1}{2\pi i}\int_{-\varepsilon}^{\varepsilon}\int_{-\varepsilon}^{\varepsilon} P_i(\underset{\sim}{X})\{\sum_\alpha A_{i\alpha}D_{\alpha j}\log(z_\alpha - c_\alpha) - \sum_\alpha \bar{A}_{i\alpha}\bar{D}_{\alpha j}\log(\bar{z}_\alpha - \bar{c}_\alpha)\}dx_1dx_2$$

where the j subscript on D_α has been added to demonstrate the associations made in section 2.2.1. Performing the integrations leads to the expression

$$\frac{1}{2\pi i} P_i(\underset{\sim}{X})\Bigg\{\sum_\alpha A_{i\alpha}D_{\alpha j}\Bigg[(x_1-c_\alpha)\left(\frac{(z_\alpha-c_\alpha)}{p_\alpha}\log(z_\alpha-c_\alpha) - x_2\right) + \frac{p_\alpha}{2}\left\{(x_2^2 - \left(\frac{x_1-c_\alpha}{p_\alpha}\right)^2)\log(z_\alpha-c_\alpha) - \left(\frac{x_1-c_\alpha}{p_\alpha}\right)\left(\frac{p_\alpha x_2^2}{2(x-c_\alpha)} - x_2\right)\right\}\Bigg] - \sum_\alpha \bar{A}_{i\alpha}\bar{D}_{\alpha j}\Bigg[(x_1-\bar{c}_\alpha)\left(\frac{(\bar{z}_\alpha-\bar{c}_\alpha)}{\bar{p}_\alpha}\log(\bar{z}_\alpha-\bar{c}_\alpha) - x_2\right) + \frac{\bar{p}_\alpha}{2}\left\{(x_2^2 - \left(\frac{x_1-\bar{c}_\alpha}{\bar{p}_\alpha}\right)^2)\log(\bar{z}_\alpha-\bar{c}_\alpha) - \left(\frac{x_1-\bar{c}_\alpha}{\bar{p}_\alpha}\right)\left(\frac{\bar{p}_\alpha x_2^2}{2(x_1-\bar{c}_\alpha)} - x_2\right)\right\}\Bigg]\Bigg\}\Bigg|_{-\varepsilon}^{\varepsilon}\Bigg|_{-\varepsilon}^{\varepsilon}$$

Substitution of the limits gives zero identically. A similar analysis on the second part of the integral

leads to

$$\frac{-1}{2\pi i}\int_{-\varepsilon}^{\varepsilon}\int_{-\varepsilon}^{\varepsilon}\phi_i(\underset{\sim}{X})\left[a_{iqkl}\left(\sum_\alpha\frac{A_{k\alpha}D_{\alpha j}}{z_\alpha-c_\alpha}-\sum_\alpha\frac{\bar{A}_{k\alpha}\bar{D}_{\alpha j}}{\bar{z}_\alpha-\bar{c}_\alpha}\right)n_q\right.$$

$$\left.+\,a_{iqk2}\left(\sum_\alpha\frac{A_{k\alpha}D_{\alpha j}}{z_\alpha-c_\alpha}\,p_\alpha-\sum_\alpha\frac{\bar{A}_{k\alpha}\bar{D}_{\alpha j}}{\bar{z}_\alpha-\bar{c}_\alpha}\,\bar{p}_\alpha\right)n_q\right]dx_1dx_2$$

Performing the indicated integrations leads to the expression

$$\frac{-1}{2\pi i}\,\phi_i(\underset{\sim}{X})\left\{a_{iqkl}\left[\sum_\alpha A_{i\alpha}D_{\alpha j}\left(\frac{(z_\alpha-c_\alpha)}{p_\alpha}\log(z_\alpha-c_\alpha)-x_2\right)\right.\right.$$

$$\left.-\sum_\alpha\bar{A}_{k\alpha}\bar{D}_{\alpha j}\left(\frac{(\bar{z}_\alpha-\bar{c}_\alpha)}{\bar{p}_\alpha}\log(\bar{z}_\alpha-\bar{c}_\alpha)-x_2\right)\right]n_q$$

$$+\,a_{iqk2}\left[\sum_\alpha A_{i\alpha}D_{\alpha j}\left(\frac{(z_\alpha-c_\alpha)}{p_\alpha}\log(z_\alpha-c_\alpha)-x_2\right)\right.$$

$$\left.\left.-\sum_\alpha\bar{A}_{k\alpha}\bar{D}_{\alpha j}\bar{p}_\alpha\left(\frac{(\bar{z}_\alpha-\bar{c}_\alpha)}{\bar{p}_\alpha}\log(\bar{z}_\alpha-\bar{c}_\alpha)-x_2\right)\right]n_q\right\}\Bigg|_{-\varepsilon}^{\varepsilon}\Bigg|_{-\varepsilon}^{\varepsilon}$$

Substituting the designated limits with appropriate n_q (i.e., $n_q = \pm 1$ on, $x = \mp\varepsilon$) and letting $\varepsilon \to 0$ gives the result which contains the constant of the integration (F) as

$$\phi_j(\underset{\sim}{x}_o)F$$

whereby (I.1) assumes the desired form of the interior identity

$$[P_i\Phi_{ij} - \Gamma_{ij}\phi_i]dS = -F\phi_j(\underset{\sim}{x}_o)$$

I.2 BOUNDARY FORMULA

To establish the boundary formula, we proceed in a similar fashion as in the interior identity development, except that rather delete the neighborhood of $\underset{\sim}{x}_o$ we augment the contour. We start with the interior identity (2.29) showing explicit point dependence

$$\int_C [P_i(\underset{\sim}{X})\Phi_{ij}(\underset{\sim}{X},\underset{\sim}{x}_o) - \Gamma_{ij}(\underset{\sim}{X},\underset{\sim}{x}_o)\phi_i(\underset{\sim}{X})]dS(\underset{\sim}{X})$$

$$= -F\phi_j(\underset{\sim}{x}_o) \qquad \text{(I.3)}$$

Augment boundary by part of a rectangle whose contour we denote C'' as shown in Figure 2. Equation (I.3) is now realized by

$$-F\phi_j(\underset{\sim}{x}_o) = \int_{C'+C''} [P_i(\underset{\sim}{X})\Phi_{ij}(\underset{\sim}{X},\underset{\sim}{x}_o)$$

$$- \Gamma_{ij}(\underset{\sim}{X},\underset{\sim}{x}_o)\phi_i(\underset{\sim}{X})]dS(\underset{\sim}{X}) \qquad \text{(I.4)}$$

Again as in the case of the interior identity, the integral over C' is identically zero, leaving only the integral over C'' to be determined. Closer examination of the contour C'' for the case when $\underset{\sim}{X}_o$ is located at a point on the boundary which does not possess a unique tangent provides geometrical relations that will be used in the establishment of the boundary formula. Figure 27 depicts this case for ε small enough that the neighboring boundary C' on either side of $\underset{\sim}{X}_o$ can be replaced with straight line segments. In accordance with contour integral direction conventions, we denote the outward unit normal of the adjacent straight line segment to $\underset{\sim}{X}_o$ in the positive contour direction sense as $\underset{\sim}{n}^+$ and the outward unit normal of the adjacent straight line segment in the negative contour direction sense as $\underset{\sim}{n}^-$. We now establish the auxiliarly cartesian coordinate system x_1'-x_2' aligned as shown in Figure 27. Specifically, x_2' is in the $-\underset{\sim}{n}_o$ direction where

$$\underset{\sim}{n}_o = \frac{\underset{\sim}{n}^+ + \underset{\sim}{n}^-}{|\underset{\sim}{n}^+| + |\underset{\sim}{n}^-|}$$

and x_1' is coincidental with the direction that the contour integration will follow along $x_2'=0$.

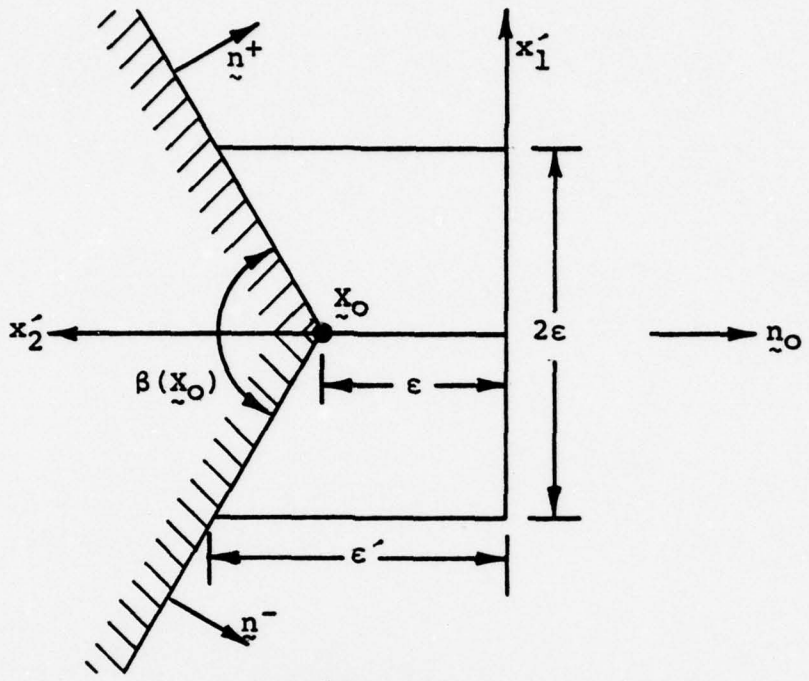

FIGURE 27

Employing this auxiliary cartesian coordinate system, the contour integral over C'' becomes

$$-F\phi_j(\underset{\sim}{x}_o) = \int_{\varepsilon'}^{0} [P_i\Phi_{ij} - \Gamma_{ij}\phi_i]dx_2' + \int_{-\varepsilon}^{\varepsilon} [P_i\Phi_{ij} - \Gamma_{ij}\phi_i]dx_1'$$

$$+ \int_{0}^{\varepsilon'} [P_i\Phi_{ij} - \Gamma_{ij}\phi_i]dx_2' \qquad (I.5)$$

where $\varepsilon' = \varepsilon(1 + \tan\frac{1}{2}(\pi-\beta(\underset{\sim}{X}_o)))$. In the first integral $x_1'=-\varepsilon$, $n_1'=-1$, $n_2'=0$, while in the second integral $x_2'=0$, $n_1'=0$, $n_2'=-1$, and in the third integral $x_1'=\varepsilon$, $n_1'=1$ and $n_2'=0$. We consider parts of the integral separately so that the first parts of the integrals in (I.5) over C'' become by the above

$$\frac{1}{2\pi i}\Bigg[\int_{\varepsilon'}^{0} P_i(\underset{\sim}{X})\{\sum_\alpha A_{i\alpha}D_{\alpha j}\log(-\varepsilon + p_\alpha x_2' - c_\alpha) - \sum_\alpha \bar{A}_{i\alpha}\bar{D}_{\alpha j}\log(-\varepsilon + \bar{p}_\alpha x_2' - \bar{c}_\alpha)\}dx_2'$$

$$+ \int_{-\varepsilon}^{\varepsilon} P_i(\underset{\sim}{X})\{\sum_\alpha A_{i\alpha}D_{\alpha j}\log(x_1' - c_\alpha) - \sum_\alpha A_{i\alpha}D_{\alpha j}\log(x_1' - c_\alpha)\}dx_1'$$

$$+ \int_{0}^{\varepsilon'} P_i(\underset{\sim}{X})\{\sum_\alpha A_{i\alpha}D_{\alpha j}\log(\varepsilon + p_\alpha x_2' - c_\alpha) - \sum_\alpha A_{i\alpha}D_{\alpha j}\log(\varepsilon + p_\alpha x_2' - c_\alpha)\}dx_2'\Bigg]$$

Performing the indicated integrations gives

$$\frac{1}{2\pi i}\Bigg[P_i(\underset{\sim}{X})\Bigg\{\sum_\alpha A_{i\alpha}D_{\alpha j}\left[\left(\frac{-\varepsilon+p_\alpha x_2'-c_\alpha}{p_\alpha}\right)\log(-\varepsilon+p_\alpha x_2'-c_\alpha)-x_2'\right] - \sum_\alpha \bar{A}_{i\alpha}\bar{D}_{\alpha j}\left[\left(\frac{-\varepsilon+\bar{p}_\alpha x_2'-\bar{c}_\alpha}{\bar{p}_\alpha}\right)\log(-\varepsilon+\bar{p}_\alpha x_2'-\bar{c}_\alpha)-x_2'\right]\Bigg\}\Bigg|_{\varepsilon'}^{0}$$

$$+ P_i(\underset{\sim}{X})\Bigg\{\sum_\alpha A_{i\alpha}D_{\alpha j}[(x_1'-c_\alpha)\log(x_1'-c_\alpha) - x_1'] - \sum_\alpha \bar{A}_{i\alpha}\bar{D}_{\alpha j}[(x_1'-\bar{c}_\alpha)\log(x_1'-\bar{c}_\alpha) - x_1']\Bigg\}\Bigg|_{-\varepsilon}^{\varepsilon}$$

$$+ P_i(\underset{\sim}{X})\Bigg\{\sum_\alpha A_{i\alpha}D_{\alpha j}\left[\left(\frac{\varepsilon+p_\alpha x_2'-c_\alpha}{p_\alpha}\right)\log(\varepsilon+p_\alpha x_2'-c_\alpha) - x_2'\right] - \sum_\alpha \bar{A}_{i\alpha}\bar{D}_{\alpha j}\left[\left(\frac{\varepsilon+\bar{p}_\alpha x_2'-\bar{c}_\alpha}{\bar{p}_\alpha}\right)\log(\varepsilon+\bar{p}_\alpha x_2'-\bar{c}_\alpha) - x_2'\right]\Bigg\}\Bigg|_{0}^{\varepsilon}\Bigg]$$

Putting in limits of integration and letting $\varepsilon \to 0$ (whereby $\varepsilon' \to 0$ also) yields zero identically.

A similar analysis on the second parts of the integrals in (I.5) gives rise to the expression

$$\frac{1}{2\pi i}\Bigg\{\int_{\varepsilon'}^{0} P_i(\underset{\sim}{X})\Bigg[a_{iqkl}\Bigg(\sum_\alpha \frac{A_{k\alpha}D_{\alpha j}}{(-\varepsilon+p_\alpha x_2'-c_\alpha)} - \sum_\alpha \frac{\bar{A}_{k\alpha}\bar{D}_{\alpha j}}{(-\varepsilon+\bar{p}_\alpha x_2'-\bar{c}_\alpha)}\Bigg)n_q' + a_{iqk2}\Bigg(\sum_\alpha \frac{A_{k\alpha}D_{\alpha j}p_\alpha}{(-\varepsilon+p_\alpha x_2'-c_\alpha)} - \sum_\alpha \frac{\bar{A}_{k\alpha}\bar{D}_{\alpha j}\bar{p}_\alpha}{(-\varepsilon+\bar{p}_\alpha x_2'-\bar{c}_\alpha)}\Bigg)n_q'\Bigg]dx_2'$$

$$+\int_{-\varepsilon}^{\varepsilon} P_i(\underset{\sim}{X})\Bigg[a_{iqkl}\Bigg(\sum_\alpha \frac{A_{k\alpha}D_{\alpha j}}{(x_1'-c_\alpha)} - \sum_\alpha \frac{\bar{A}_{k\alpha}\bar{D}_{\alpha j}}{(x_1'-\bar{c}_\alpha)}\Bigg)n_q' + a_{iqk2}\Bigg(\sum_\alpha \frac{A_{k\alpha}D_{\alpha j}}{(x_1'-c_\alpha)} - \sum_\alpha \frac{\bar{A}_{k\alpha}\bar{D}_{\alpha j}}{(x_1'-\bar{c}_\alpha)}\Bigg)n_q'\Bigg]dx_1'$$

$$+\int_{0}^{\varepsilon'} P_i(\underset{\sim}{X})\Bigg[a_{iqkl}\Bigg(\sum_\alpha \frac{A_{k\alpha}D_{\alpha j}}{(\varepsilon+p_\alpha x_2'-c_\alpha)} - \sum_\alpha \frac{\bar{A}_{k\alpha}\bar{D}_{\alpha j}}{(\varepsilon+\bar{p}_\alpha x_2'-\bar{c}_\alpha)}\Bigg)n_q' + a_{iqk2}\Bigg(\sum_\alpha \frac{A_{k\alpha}D_{\alpha j}p_\alpha}{(\varepsilon+p_\alpha x_2'-c_\alpha)} - \sum_\alpha \frac{\bar{A}_{k\alpha}\bar{D}_{\alpha j}\bar{p}_\alpha}{(\varepsilon+\bar{p}_\alpha x_2'-\bar{c}_\alpha)}\Bigg)n_q'\Bigg]dx_2'\Bigg\}$$

Performing the indicated integrals gives

AD-A057 304 KENTUCKY UNIV LEXINGTON DEPT OF ENGINEERING MECHANICS F/G 12/1
THE BOUNDARY INTEGRAL EQUATION METHOD FOR THE NUMERICAL SOLUTIO--ETC(U)
APR 78 M L SCHULOCK AFOSR-75-2824

UNCLASSIFIED UKY-TR107-78-EM16 AFOSR-TR-78-1184 NL

2 OF 2
ADA
057304

END
DATE
FILMED
9-78
DDC

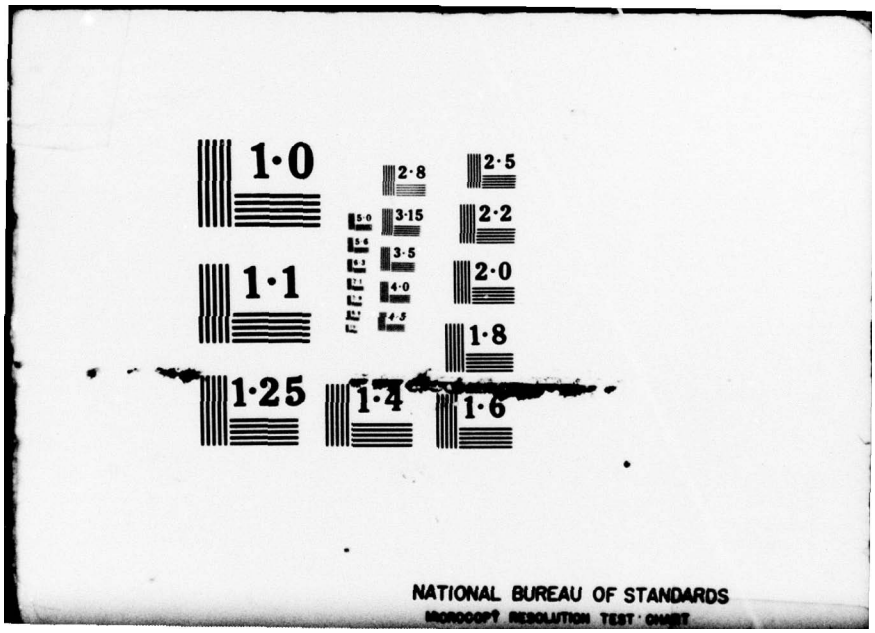
1·0
1·1
1·25
2·8
3·15
3·5
4·0
4·5
1·4
2·5
2·2
2·0
1·8
1·6
NATIONAL BUREAU OF STANDARDS
MICROCOPY RESOLUTION TEST CHART

$$\frac{1}{2\pi i}\Bigg\{P_i(\underset{\sim}{X})\Bigg[a_{iqk1}\Bigg(\sum_\alpha \frac{A_{k\alpha}D_{\alpha j}}{p_\alpha}\log(-\varepsilon+p_\alpha x_2'-c_\alpha) - \sum_\alpha \frac{\bar{A}_{k\alpha}\bar{D}_{\alpha j}}{\bar{p}_\alpha}\log(-\varepsilon+\bar{p}_\alpha x_2'-\bar{c}_\alpha)\Bigg) n_q' + a_{iqk2}\Bigg(\sum_\alpha A_{k\alpha}D_{\alpha j}\log(-\varepsilon+p_\alpha x_2'-c_\alpha) - \sum_\alpha \bar{A}_{k\alpha}\bar{D}_{\alpha j}\log(-\varepsilon+\bar{p}_\alpha x_2'-\bar{c}_\alpha)\Bigg) n_q'\Bigg]\Bigg|_{\varepsilon'}^{0}$$

$$+ P_i(\underset{\sim}{X})\Bigg[a_{iqk1}\Bigg(\sum_\alpha A_{k\alpha}D_{\alpha j}\log(x_1'-c_\alpha) - \sum_\alpha \bar{A}_{k\alpha}\bar{D}_{\alpha j}\log(x_1'-\bar{c}_\alpha)\Bigg) n_q' + a_{iqk2}\Bigg(\sum_\alpha A_{k\alpha}D_{\alpha j}p_\alpha\log(x_1'-c_\alpha) - \sum_\alpha \bar{A}_{k\alpha}\bar{D}_{\alpha j}\bar{p}_\alpha\log(x_1'-\bar{c}_\alpha)\Bigg) n_q'\Bigg]\Bigg|_{-\varepsilon}^{\varepsilon}$$

$$+ P_i(\underset{\sim}{X})\Bigg[a_{iqk1}\Bigg(\sum_\alpha \frac{A_{k\alpha}D_{\alpha j}}{p_\alpha}\log(\varepsilon+p_\alpha x_2'-c_\alpha) - \sum_\alpha \frac{\bar{A}_{k\alpha}\bar{D}_{\alpha j}}{\bar{p}_\alpha}\log(\varepsilon+\bar{p}_\alpha x_2'-\bar{c}_\alpha)\Bigg) n_q' + a_{iqk2}\Bigg(\sum_\alpha A_{k\alpha}D_{\alpha j}\log(\varepsilon+p_\alpha x_2'-c_\alpha) - \sum_\alpha \bar{A}_{k\alpha}\bar{D}_{\alpha j}\log(\varepsilon+\bar{p}_\alpha x_2'-\bar{c}_\alpha)\Bigg) n_q'\Bigg]\Bigg|_{0}^{\varepsilon'}\Bigg\}$$

Substituting the designated limits with the appropriate n_q' and letting $\varepsilon \to 0$ (while $\varepsilon' = \varepsilon(1+\tan\frac{1}{2}(\pi-\beta(\underset{\sim}{X}_o)))$

leads to the result

$$(\beta(\underset{\sim}{X}_o) - 1)F\phi_j(\underset{\sim}{X}_o)$$

Thus by this result in (I.5) we arrive at the boundary integral equation

$$-\lambda_{ij}(\underset{\sim}{X}_o)F\phi_i(\underset{\sim}{X}_o) = \int_C [P_i(\underset{\sim}{X})\Phi_{ij}(\underset{\sim}{X},\underset{\sim}{X}_o) - \Gamma_{ij}(\underset{\sim}{X},\underset{\sim}{X}_o)\phi_i(\underset{\sim}{X})]ds(\underset{\sim}{X})$$

where $\lambda_{ij}(\underset{\sim}{X}_o)$ represents the addition of the result of the contour integration over C'' and the left hand side of equation (I.5).

APPENDIX II

CALCULATION OF ELEMENTS OF COEFFICIENT MATRIX IN POLYNOMIAL SHAPE FUNCTION APPROXIMATION

II.1 CALCULATION OF $a_{ij}^{\alpha\sigma}$ AND $F\lambda_{ij}^{\sigma}$

We defined $a_{ij}^{\alpha\sigma}$ and $F\lambda_{ij}^{\sigma}$ in section 2.3.4 in equations (2.43) and (2.44) as

$$a_{ij}^{\alpha\sigma} = \int_{C_\sigma} M^{\alpha}(\xi)\Gamma_{ij}(\underset{\sim}{X}(\xi), \underset{\sim}{X}_o)J(\xi)d\xi$$

$$F\lambda_{ij}^{\sigma} = \int_{C_\sigma} \Gamma_{ij}(\underset{\sim}{X}(\xi), \underset{\sim}{X}_o)J(\xi)d\xi$$

with Γ_{ij} in the form as given by (3.23), viz.

$$\Gamma_{ij}(\underset{\sim}{X}(\xi), \underset{\sim}{X}_o) = \frac{1}{2\pi i}\left[\sum_{\alpha}\frac{L_{ik\alpha}D_{\alpha j}}{[X_1(\xi) + p_\alpha X_2(\xi) - (a+p_\alpha b)]}\right.$$

$$\left. - \sum_{\alpha}\frac{\bar{L}_{ik\alpha}\bar{D}_{\alpha j}}{[X_1(\xi) + \bar{p}_\alpha X_2(\xi) - (a+\bar{p}_\alpha b)]}\right]n_k$$

Now Γ_{ij} in this form has a $O(\frac{1}{\xi})$ singularity at the point $\underset{\sim}{c}_\alpha = \underset{\sim}{z}_\alpha(\xi)$ which suggests that we handle the necessary integrations on the basis of whether the singularity exists on the segment C_σ over which we are integrating. Accordingly, we can classify these integrals as either of the two cases:

1. $\underset{\sim}{X}_o$ is not an element of C_σ
2. $\underset{\sim}{X}_o$ is an element of C_σ

(i) For the first case, there is no singularity on C_σ and the integrals can be evaluated approximately by the ν-point Gaussian quadrature rule given by (2.38). Thus,

$$a_{ij}^{\alpha\sigma} \doteq [\sum_{k=1}^{\nu} w_k \{M^\alpha(\xi_k)\Gamma_{ij}(\underset{\sim}{X}(\xi_k), \underset{\sim}{X}_o)J(\xi_k)\}]\Delta\xi$$

$$F\lambda_{ij}^{\sigma} \doteq [\sum_{k=1}^{\nu} w_k \{\Gamma_{ij}(\underset{\sim}{X}(\xi_k), \underset{\sim}{X}_o)J(\xi_k)\}]\Delta\xi$$

in which $\Delta\xi=2$.

(ii) For a polynomial shape function approximation, the occurence of $\underset{\sim}{X}_o$ as an element of C_α is recognized as the case of $\underset{\sim}{X}_o$ being one of the local nodes (α) of C_α.

Presupposing that $\phi_i(\underset{\sim}{X}_o)$ is known, the behavior of the left hand side of equation (2.39) may be observed according to the location of $\underset{\sim}{X}_o$. Specifically we want to show that the quantity

$$\phi_i(\underset{\sim}{X}) - \phi_i(\underset{\sim}{X}_o)$$

is $O(r)$ ($O(\xi)$ in the mapped space) so that the integrand of the left hand side of (2.39) is non-singular since we know $\Gamma_{ij}(\underset{\sim}{X}, \underset{\sim}{X}_o)$ is $O(\frac{1}{r})$ ($O(\frac{1}{\xi})$ in the mapped space as was observed in the previous case). The polynomial shape

functions are of the general form

$$M^{\alpha}(\xi) = a^{\alpha} + b^{\alpha}\xi + c^{\alpha}\xi^2 + \ldots$$

Denote the value of ξ at the local node (α) at which $\underset{\sim}{X}_o$ is located as $\xi(\alpha)$. By equation (2.33)

$$\phi_i(\underset{\sim}{X}) - \phi_i(\underset{\sim}{X}_o) = (a^{\alpha} + b^{\alpha}\xi + c^{\alpha}\xi^2 + \ldots)\phi_i^{\alpha\sigma}$$

$$- (a^{\alpha} + b^{\alpha}\xi(\alpha) + c^{\alpha}\xi^2(\alpha) + \ldots)\phi_i^{\alpha\sigma}$$

which is $O(\xi)$. We may rewrite this quantity as

$$\phi_i(\underset{\sim}{X}) - \phi_i(\underset{\sim}{X}_o) = \phi_i^{\alpha\sigma}[M^{\alpha}(\xi) - M^{\alpha}(\xi(\alpha))]$$

and modify equation (2.41) as

$$\sum_{\sigma=1}^{m} \phi_i^{\alpha\sigma}[M^{\alpha}(\xi) - M^{\alpha}(\xi(\alpha))](a_{ij}^{\alpha\sigma} - F\lambda_{ij}^{\sigma}) = \sum_{\sigma=1}^{m} P_i^{\alpha\sigma} b_{ij}^{\alpha\sigma}$$

Define

$$\bar{a}_{ij}^{\alpha\sigma} = [M^{\alpha}(\xi) - M^{\alpha}(\xi(\alpha))](a_{ij}^{\alpha\sigma} - F\lambda_{ij}^{\sigma})$$

as the non-singular matrix element to be evaluated by the ν-point Gaussian quadrature rule.

II.2 CALCULATION OF $b_{ij}^{\alpha\sigma}$

The matrix element $b_{ij}^{\alpha\sigma}$ was defined in section 2.3.4 by equation (2.45) as

$$b_{ij}^{\alpha\sigma} = \int_{C_\sigma} M^\alpha(\xi)\Phi_{ij}(\underset{\sim}{X}(\xi),\underset{\sim}{X}_o)J(\xi)d\xi$$

with

$$\Phi_{ij}(\underset{\sim}{X}(\xi),\underset{\sim}{X}_o) = \frac{1}{2\pi i}\{\sum_\alpha A_{k\alpha}D_{\alpha j}\log(X_1(\xi)+p_\alpha X_2(\xi)-(a+p_\alpha b))$$

$$- \sum_\alpha \bar{A}_{k\alpha}\bar{D}_{\alpha j}\log(X_1(\xi)+\bar{p}_\alpha X_2(\xi)-(a+\bar{p}_\alpha b))\}$$

As in the previous section, there is a singularity present in the kernel, which in this case of $\Phi_{ij}(\underset{\sim}{X}(\xi),\underset{\sim}{X}_o)$ is log (ξ). Again we separate cases of the above integration on the basis of whether $\underset{\sim}{X}_o$ is an element of C_σ.

(i) The singularity does not exist on the segment C_σ and $b_{ij}^{\alpha\sigma}$ can be evaluated by the ν-point Gaussian quadrature rule as

$$b_{ij}^{\alpha\sigma} \doteq [\sum_{k=1}^{\nu} w_k\{M^\alpha(\xi_k)\Phi_{ij}(\underset{\sim}{X}(\xi_k),\underset{\sim}{X}_o)J(\xi_k)\}]\Delta\xi$$

where $\Delta\xi=2$.

(ii) The order of the singularity is log(ξ) and the integral cannot be evaluated in the normal sense. To deal with the situation we subdivide the segment C_σ

into γ subintervals (where γ is the degree of the polynomial shape function in the approximation) and integrate by an appropriate numerical procedure over the subintervals according to whether $\underset{\sim}{X}_o$ is a member of the subinterval.

Denote the subintervals τ_ω^σ which are defined as

$$\tau_\omega^\sigma = [\xi(\omega), \xi(\omega+1)] \qquad \omega=1,2,\ldots\gamma$$

in which $\xi(\omega)$ is interpreted as the value of ξ at local node number ω and $\xi(\omega+1)$ the value of ξ at local node number $\omega+1$. We now have

$$b_{ij}^{\alpha\sigma} = \sum_{\omega=1}^{\gamma} \int_{\tau_\omega^\sigma} M^\alpha(\xi) \Phi_{ij}(\underset{\sim}{X}(\xi), \underset{\sim}{X}_o) J(\xi) d\xi$$

Transform the Gaussian abcissae ξ to be in the interval τ_ω^σ by

$$\zeta = \frac{[\xi(\omega)+\xi(\omega+1)] - [\xi(\omega+1)-\xi(\omega)]}{2}$$

We now may approximately evaluate $b_{ij}^{\alpha\sigma}$ as

$$b_{ij}^{\alpha\sigma} \doteq \sum_{\omega=1}^{\gamma} [\sum_{k=1}^{\nu} w' \{M^\alpha(\zeta_k) \Phi_{ij}(\underset{\sim}{X}(\zeta_k), \underset{\sim}{X}_o) J(\zeta_k)\}] \Delta\zeta$$

where

$$\zeta_k = \frac{[\xi(\omega)+\xi(\omega+1)] - [\xi(\omega+1)-\xi(\omega)]\xi_k}{2}$$

$$\Delta\zeta = \xi(\omega+1) - \xi(\omega)$$

$$w_k' = \frac{\Delta\zeta}{2} w_k$$

If $\underset{\sim}{X}_o \in \tau_\omega^\sigma$ we then replace w_k' by the log weighting function [15]

$$w_k' = \log\sqrt{(\zeta_k - \xi(\underset{\sim}{X}_o))^2}$$

where $\xi(\underset{\sim}{X}_o)$ is the value of ξ at which $\underset{\sim}{X}_o$ is located.

APPENDIX III

CALCULATION OF BOUNDARY STRESSES

The mapping of the contour C to ξ space does not allow the approximation of $\partial u_i/\partial X_j$ directly because we cannot obtain an expression for $\partial \xi/\partial X_j$ (cf. section 2.3.2). Consequently, we must establish a secondary system of linear equations to evaluate boundary values of σ_{ij} that cannot be determined from the traction solution. Thereafter, Mohr's Circle can be used to evaluate oblique stresses such as the hoop stress. The order of the linear system established is dependent on the number of components (N) in the problem for which appropriate values of indices will be assigned subsequently.

For the problem of anisotropic elasticity the fundamental variables (ϕ_i) are displacements (u_i) while the flux-type variables (P_i) are tractions (t_i). An analysis of stress gives the relation [17]

$$t_i = \sigma_{ij} n_j \qquad \begin{matrix} i = 1,2,\ldots N \\ j = 1,2 \end{matrix}$$

which represents N equations in 2N unknowns (σ_{ij}). However, the anlaysis of stress also provides that

$$\sigma_{ij} = \sigma_{ji}$$

so that there are actually only 2N-1 unknowns.

The assumption of small strains (Eulerian strain tensor) allows formulation of N additional equations. The Eulerian strain tensor ϵ_{ij} takes the form

$$\epsilon_{ij} = \frac{1}{2}\left(\frac{\partial u_i}{\partial x_j} + \frac{\partial u_j}{\partial x_i}\right)$$

The PSFBIE provides that by equation (2.33) the pertinent boundary variables take the form

$$u_i = M^{\alpha}(\xi) u_i^{\alpha} \qquad i = 1,2,\ldots N$$

$$X_j = M^{\alpha}(\xi) X_j^{\alpha} \qquad j = 1,2$$

By the chain rule for differentiation the derivative of the displacements with respect to the mapped coordinate (ξ) can be expressed as

$$\frac{\partial u_i}{\partial \xi} = \frac{\partial u_i}{\partial X_j} \frac{\partial X_j}{\partial \xi}$$

Now the quantities $\partial u_i/\partial \xi$ and $\partial X_j/\partial \xi$ can be approximated by use of the shape functions (M^{α}) as

$$\frac{\partial u_i}{\partial \xi} = \frac{\partial M^{\alpha}(\xi)}{\partial \xi} u_i^{\alpha}$$

$$\frac{\partial X_j}{\partial \xi} = \frac{\partial M^{\alpha}(\xi)}{\partial \xi} X_j^{\alpha}$$

Thus we have established N equations in the 2N unknowns $\partial u_i/\partial x_j$. Note that analysis of strain provides that $\epsilon_{ij} = \epsilon_{ji}$ but not $\partial u_i/\partial x_j = \partial u_j/\partial x_i$, so that at this point we have 2N equations in 4N-1 unknowns.

Examination of the constitutive relation (Hooke's Law) provides the additional 2N-1 equations in the proper 4N-1 unknowns necessary to complete the linear system. Hooke's Law is

$$\sigma_{ij} = c_{ijk\ell}\epsilon_{k\ell} \qquad \begin{matrix} i,k = 1,2,\ldots N \\ j,\ell = 1,2 \end{matrix}$$

where $\epsilon_{k\ell}$ is the Eulerian strain tensor. Using the interpretation of $\epsilon_{k\ell}$ given above yields

$$\sigma_{ij} = c_{ijk\ell}\left(\frac{\partial u_k}{\partial x_\ell} + \frac{\partial u_\ell}{\partial x_k}\right)$$

which may be recognized as the required additional 2N-1 equations in the proper 4N-1 unknowns.

Solution of the indicated linear system yields values of the stresses at the boundary point in question which may be rotated through the necessary angles to determine the stresses of interest.

REFERENCES

[1] Zienkiewicz, O.C., The Finite Element Method In Engineering Science, McGraw-Hill, Inc.,1971.

[2] Clements, D.L. and Rizzo, F.J., "An Algorithm for The Numerical Solution of Boundary Value Problems Governed by Second Order Elliptic Systems", (in review for publication).

[3] Eshelby, J.D., Reed, W.T., and Shockley, W., "Anisotropic Elasticity with Application to Dislocation Theory", Acta Metallurgica, Vol. 1, May, 1953, pp.251-259.

[4] Stroh, A.N., "Dislocations and Cracks in Anisotropic Elasticity", Philosophical Magazine, Vol. 3, June, 1958, pp.625-646.

[5] Ralston, A., A First Course in Numerical Analysis, McGraw-Hill, Inc., 1965.

[6] Lekhnitskii, S.G., Anisotropic Plates, Gordon and Breach, Inc., 1968.

[7] Cruse, T.A. and Rizzo, F.J., editors, Boundary Integral Equation Method, Computational Applications in Applied Mechanics, ASME Proceedings AMD-Vol. II, 1975.

[8] Cruse, T.A. and Lachat, J.C., editors, Proceedings of The International Symposium on Innovative Numerical Analysis in Applied Engineering Science, Versailles, France, 1977.

[9] Wu, Y.S., The Boundary Integral Equation Method Using Various Approximation Techniques for Problems Governed by Laplace's Equation, AFOSR-TR-1313, December, 1976.

[10] Fairweather, G., Rizzo, F.J., Shippy, D.J., and Wu, Y.S., On the Numerical Solution of Two-Dimensional Potential Problems by an Improved Boundary Integral Equation Method (manuscript).

[11] Conte, S.D. and deBoor, C., Elementary Numerical Analysis, 2nd ed., McGraw-Hill, Inc., 1972.

[12] Rizzo, F.J. and Shippy. D.J., "A Method for Stress Determination in Plane Anisotropic Elastic Bodies", J. Composite Materials, Vol. 4, January, 1970, pp.36-61.

[13] Green, A.E., "A Note on Stress Systems in Aeolotropic Materials", Philosophical Magazine, Vol. 34, 1943, pp.416-422.

[14] Cruse, T.A. and Swedlow, J.L., Interactive Program for Analysis and Design Problems in Advanced Composites Technology, AFML-TR-71-268, December, 1971.

[15] Lekhnitskii, S.G., Theory of Elasticity of an Anisotropic Elastic Body, Holden-Day, Inc., 1963.

[16] Stroud, A.H. and Secrest, D., Gaussian Quadrature Formulas, Prentice-Hall, Inc., 1966.

[17] Sokolnikoff, I.S., The Mathematical Theory of Elasticity, 2nd ed., McGraw-Hill, Inc., 1956.